# A review of small heat pipes for electronics

Chen, Xianping; Ye, H; Fan, Xuejun; Ren, Tianling; Zhang, Guo Qi

**DOI**
10.1016/j.applthermaleng.2015.11.048

**Publication date**
2016

**Document Version**
Accepted author manuscript

**Published in**
Applied Thermal Engineering

# A review of small heat pipes for electronics

Xianping Chen[1,3,4 *], Huaiyu Ye[2,4 *,+], Xuejun Fan[5],Tianling Ren[1], Guoqi Zhang[2]

[1]Institute of Microelectronics, Tsinghua University, 100084 Beijing, China

[2]Electronic Components, Technology and Materials, Delft University of Technology, Delft 2628 CD, The Netherlands

[3]Faculty of Electromechanical Engineering, Guilin University of Electronic Technology, Guilin 541004, China

[4]State Key Laboratory of Solid-State Lighting, Haidian, Beijing 100086, China

[5]Department of Mechanical Engineering, Lamar University, Beaumont, TX, USA

*These authors contributed equally to this work and should be considered co-first authors

[+]Corresponding authors: Huaiyu Ye, h.ye@tudelft.nl;

**Abstract**

Heat pipes (HPs) have received considerable attention in recent decades especially in the realm of cooling electronics, which requires removing increasing heat from an area of limited volume to the environment. Small HPs are widely used in electronics applications, which are normally limited by the compact structure and dimensions. Among small HPs, mini/micro HPs and two-phase loops (TPLs) with mini/micro wicks, including loop HP (LHPs) and capillary pumped loops (CPLs) are preferred for their high efficiency, small dimension, and compatible process with semiconductor devices. TPLs in particular possess all of the main advantages of traditional HPs with the addition of special properties to transfer heat for distances of up to several meters at any orientation in the gravity field. Further, small vapour chambers (VCs), also referred to as flat HPs, are excellent candidates for electronic heat spreaders due to their light weight, geometric flexibility, and extremely high thermal conductivities. Because silicon is widely used in electronics, it is highlighted as one a preferred material for mini/micro HPs as well as TPLs. Moreover, polymer-based small HPs are highly attractive for further development because they are both cheap and easy to fabricate. Because the smaller wicks supply a greater capillary force, nano wicks such as the carbon nanotube (CNT) may represent the future of HPs due to their potentially outstanding characteristics. In this work, a review of small HPs covering design, analysis, and fabrication is presented.

Keywords: small heat pipes; electronic cooling; micro wicks; nano wicks.

## Contents


1. **Introduction** ........ - 4 -
2. **Mini/Micro heat pipes for electronics** ........ - 6 -
    - 2.1. Mini/Micro heat pipes ........ - 6 -
    - 2.2. From small to micro ........ - 7 -
    - 2.3. Wicks in mini/micro heat pipes ........ - 8 -
3. **Small two-phase loops for electronics** ........ - 11 -
    - 3.1. Loop heat pipes and capillary pumped loops ........ - 11 -
    - 3.2. Principles of loop heat pipes ........ - 13 -
    - 3.3. From small to micro ........ - 15 -
4. **Small vapour chambers for electronics** ........ - 20 -
    - 4.1. Vapour chambers ........ - 20 -
    - 4.2. Nano wicks in vapour chambers ........ - 21 -
5. **Configurations and fabrication** ........ - 23 -
    - 5.1. Materials ........ - 23 -
    - 5.2. Structure, fabrication and process ........ - 26 -
    - 5.3. Working fluids ........ - 29 -
    - 5.4. Limitations ........ - 32 -
6. **Summary and discussion** ........ - 33 -
7. **Prospective and conclusion** ........ - 36 -

**Acknowledgments** ........ - 37 -

**References** ........ - 38 -

## 1. Introduction

In recent decades, more and more power dissipation and consequently more heat has been introduced into electronic systems due to decreasing chip size, increasing device density and faster circuit speeds. Moreover, emerging developed semiconductor devices such as Radio Frequency (RF) systems, high power Light-Emitting Diodes (LEDs), solar cells and solid-state laser light sources have all suffered large on-chip temperature gradients due to localized high heat flux resulting from the substantial non-uniformity in power dissipation [1-6]. To solve the heat problems, which include but are not limited to electronic systems, Marcinichen et al. [7, 8] suggested primarily four competing technologies for the cooling of chips: microchannel single-phase flow, porous media flow, jet impingement cooling, and microchannel two-phase flow. These technologies can be categorized into two types: passive and active cooling. Passive solutions are always preferred due to their advantages in waste energy recovery. A heat pipe (HP) is a simple device working with cooling fluid and an energy recovery unit to use the waste heat generated by electronics to drive the cooling fluids. HPs can also be defined as a passive cooling device with a two-phase flow that can obtain self-drive without an external power input. HPs have been used for many years due to their high thermal conductivity, high efficiency without extra electric energy consumption, and suitable working temperature for electric devices. Their application to electronics is usually limited by the compact structure and dimensions of electronic devices. Therefore, those HPs used for the cooling of electronics are mostly defined as micro/mini HPs according to definitions that rely on the hydraulic diameter $D_h$ by Mehendale et al. [9] and Kandlikar [10]. In general, a size classification is defined as follows [11, 12]: micro-channels (50 to 600 $\mu$m), mini-channels (600 $\mu$m to 3 mm) and conventional channels ($D_h$ > 3 mm).

The trend toward miniaturization is becoming increasingly obvious for HPs to approach the heat source as closely as possible, obtain higher contact surface and enhance capillary force. HPs with micro-wicks or microgrooves, which require micro-fabrication and new materials, are booming. As the technology has progressed, HPs have also changed structurally, as in the separation of wicks and tubes. Two-phase loops

(TPLs) including loop heat pipes (LHPs) and capillary pump loop (CPLs) have attracted increasing interest since their invention due to their special properties to transfer heat for distances of up to several meters at any orientation in the gravity field. Vapour chambers (VCs) have also been mentioned as flat HPs with micro grooves. More recently, silicon has been highlighted as the best material with which to replace metals due to its fabricability and compatibility with semiconductor devices; however, other materials remain highly attractive for variant applications. Traditionally, metals have remained under investigation to make micro wicks with continuous improvement; further, polymer based HPs are highly attractive due to their flexibility and low cost, especially for LHPs and VCs. Moreover, new, exciting materials for cooling electronics, such as the nano-wick VCs have been introduced and highlighted. The carbon nanotube (CNT) in particular may represent the future of nano wicks because of its potentially outstanding characteristic to miniaturize the wicks of HPs from micro to nano scale. In this review, we define HPs on any small, hot device, especially electronics, as small HPs with mini/micro channels and wicks. An overview of the rapid progress of small HPs in terms of design, analysis and fabrication is provided below.

Small HPs typically use mini/micro wicks or channels to supply capillary force and small tubes to transfer heat to the condenser. The tube design is based on the dimension, gravity-affected length and total transferred heat. The hydraulic diameter of HPs is not usually a suitable criterion for small HPs, although they may be in some cases. For example, in many small HPs using triangular or rectangular wicks tips, the equivalent $D_h$ in the wicks is at micro level while the tube is rather larger. As shown in Table 1, small HPs include traditional types with mini/micro wicks (referred to as mini/micro HP), small TPLs, small VCs, and small flat HPs with mini/micro wicks are listed. In this work, HP is either the generally name for all two-phase capillary thermal control devices or a specific name for the traditional HPs invented in 1892 [19, 20], excluding LHPs, CPLs, VCs, etc. Specifically, we still use the term MHPs, a widely used term for HPs with micro wicks and mini/micro tubes in many references. MHPs are small scale devices that are used to cool microelectronic chips with a hydraulic diameter on the order of 10 to 500 $\mu$m [13]. MLHPs and MCPLs are also referred to as LHPs and CPLs with micro wicks.

**Table 1. Comparison of mini/micro HPs, small TPLs and small VCs**

| | Configurations | Wick Materials | Characteristics |
|---|---|---|---|
| Mini/ Micro HPs | Mini/Micro channel | Metal, Silicon | Integration of wicks, evaporator, condenser and tubes; |
| | Mini/Micro wick | Metal, Silicon and Metal, Porous media | Sintered, groove, or mesh wicks along the tubes; |
| Small TPLs | Loop heat pipe | Metal, Silicon, Polymer | Integration of wicks and evaporator; Separated condenser and tubes; Wicks are separated from tubes; |
| | Capillary pumped loop | | |
| Small VCs/ Flat HPs | | Metal, Polymer, Silicon, Porous media, CNT | Integration of wicks, evaporator and condensation chamber; Flat structure; |

## 2. Mini/Micro heat pipes for electronics

### *2.1. Mini/Micro heat pipes*

An HP is a device for heat transfer with phase change and no moving parts [14-16]. It is composed of three sections: the evaporator section, the condenser section and the adiabatic section in between [17, 18]. An HP can transport large quantities of heat efficiently from an evaporator to a condenser, but it cannot be a complete cooling system without the combination of natural or forced-air cooling [19]. Its capability results from the latent heat of working fluids and the capillary force through the wicks. For electronics, the diameters of MHPs are in the centimetre to millimetre range, but with micro size wicks. Figure 1(a) shows the typical metallic tubular HP with microgrooves (the equivalent $D_h$ calculated from the U-shaped wicks) [20]. Figure 1(b) shows the typical silicon triangle MHP (the equivalent $D_h$ calculated from the tips of the triangle). Unlike conventional HPs, the wicks in silicon MHPs can be replaced by the tip of the triangle, rectangle or pentagram [21].

(a) (b)
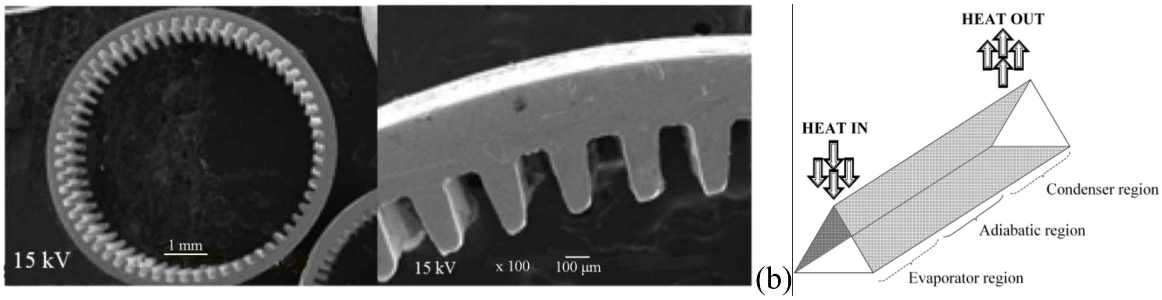


**Figure 1. Typical micro heat pipes: (a) metallic tubular MHP [20] (b) silicon triangle MHP [17].**

*2.2. From small to micro*

**Figure 2. Micro-grooved heat pipe and its grooves [22].**

As discussed above, the application of HPs in electronic devices is limited by the devices' compact structures and dimensions. Thus, MHPs are better for those relatively small structures. Li et al. [22] made great progress in traditional HP technology for high heat-flux electronic products. As shown in Figure 2, micro grooves with a depth of 0.2-0.3 mm and top-width-to-depth ratio of 1.2-1.5 were fabricated along the metallic MHP. They also built capillary limit models for MHPs with dovetail-groove, rectangular-groove, trapezoidal-groove and V-groove wick structures for theoretical analysis. Many MHPs also use sintering techniques to process particulate materials, aiming to fabricate porous media[23, 24]. Those particles have an equivalent spherical diameter of approximately 100 µm, which forms many micro channels.

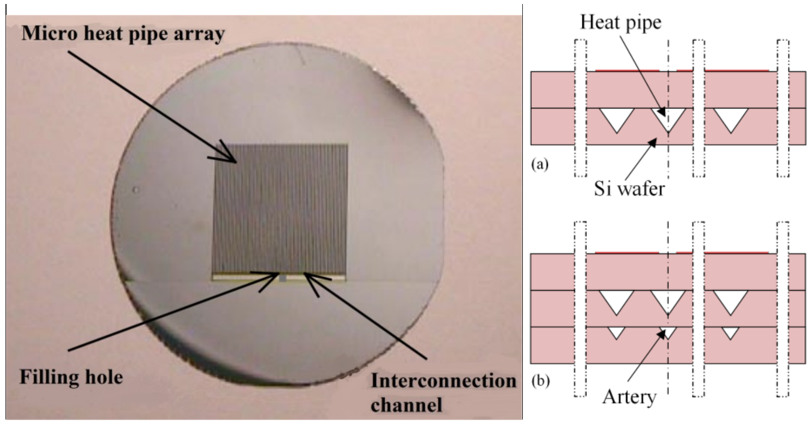


**Figure 3. Layout of the MHP array with 55 "V" grooves micromachined in a silicon wafer with triangle and artery channels [25].**

To directly cool a semiconductor device, researchers have been using silicon to manufacture the MHPs [13, 26-28]. As shown in Figure 3, Berre et al. [25] developed an effective thermal conductivity of 600 W/mK MHP for cooling electronics consisting of a series of 55 parallel triangular-shaped channels. The working fluids for cooling the poly silicon heater were ethanol and methanol. The temperature difference between the evaporator and the condenser finally reached 4.7ºC and was only 1.6ºC when the HP array was empty; however, the MHPs cannot function properly without a heat sink. McGlen et al. [29] have developed a system using MHP and loop thermosyphon technology to maintain chip operational temperatures of <70ºC at an ambient air temperature of 55ºC. The prototype combined micro and mini HPs with force convection cooling to increase the total manageable power of each unit to 230 W, which gives a total rack power of approximately 8 kW.

*2.3. Wicks in mini/micro heat pipes*

Smaller channels are desirable for two reasons: (1) the higher heat transfer coefficient, and (2) higher heat transfer surface area per unit flow volume. In fact, new cooling techniques in MHPs are being attempted to dissipate heat fluxes in electronic components on the order of 100 to 1000 W/cm$^2$ [30]. As shown in Figure 4, heat added to the evaporator region of the HP results in the vaporization of the working fluid; consequently, the high temperature and associated high pressure induces vapour flow to the condenser region where it is condensed, releasing the latent heat of the working fluid. Liquid can be transported through the sharp angled corner regions by the capillary pressure. Babin et al. [31] undertook the first theoretical analysis and experiment on MHPs. Moreover, Khrustalev and Faghri [32] proposed a numerical model of the heat and mass transfer occurring in an MHP including the effects of shear stresses at the liquid-vapour interface. These and several other models have been summarized in detail and the results compared by Peterson et al. [28, 33]. Additionally, the approximate analytical approach of Cotter [34] has been re-evaluated with currently available experimental data to modify the approach to better predict the actual operating conditions and maximum heat transport capacity. Wang et al. [35] reported that this new model better approximates the physical behaviour of the liquid-vapour interface in the dryout region. A 3D numerical model was later developed to simulate the MHP. The results of Mallik et al. [27] indicate that significant reductions in the maximum chip temperature, thermal gradients and localized heat fluxes can be obtained through the incorporation of MHP arrays. Rahmat and Hubert [36] applied a two-phase model of a single MHP and a 3D network of micro-channels simulated using the finite element method. Wire-bonded MHP arrays were analysed by Wang et al. and Launay et al. [37-39]. Tests of metallic MHPs were conducted by Yong et al. [20, 40] and Kang et al. [41, 42]. They developed their design based on over-analysis with analytical solution or simulation results.

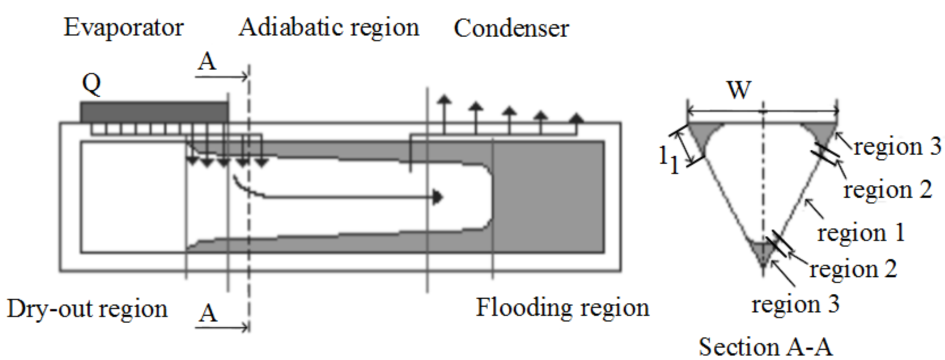


**Figure 4. Micro heat pipe with triangular capillary microchannels [13, 30].**

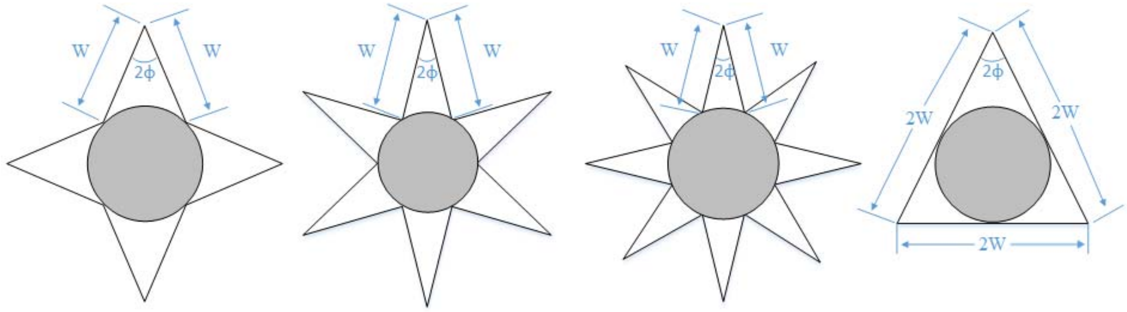


**Figure 5. Geometry of different cross-sectional shape of micro-heat pipes [43].**

As discussed above, conventional metallic MHPs still use micro grooves as wicks, as shown in Figure 1(a). In general, gravity and capillarity are the most important parameters in tubular MHPs, where they act as the drive force. They are fully driven by the capillary force, which depends mainly on the wicks but is negatively affected by gravity. Li et al. [20] reported that metallic MHPs with a 6mm diameter (trapezium-grooved wick with 60 teeth) can achieve 100 times the heat conduction coefficient of copper. Li et al. [22] recommended that MHPs with the grooved wick of a small-angle dove-tailed structure or a rectangular or small-angle trapezoidal structure be employed to obtain better heat transfer performances. Further, it has been shown that in MHPs with a compound structure of a sintered wick on a trapezium-grooved substrate [44], the capillary limit decreases with the particle size of copper powders, and learning how to reduce the backflow resistance of working fluid is crucial to increasing capillary limits. A report about the collapse in flattening a micro-grooved HP was conducted by Li et al. [40], who found that clearance between the tube and plates occurs at room temperature. As the temperature increases, the incidence of wall collapse decreases until it finally disappears, and the critical temperature is approximately 130°C for various heights of flattened HPs. Murer et al. [45] have developed experimental and numerical analyses of the transient response of a mini/micro HP. The analytical model was validated by the tested samples, which were copper-water flat HPs with a rectangular cross section ($10 \times 2.1$ mm$^2$) and cylindrical HPs (diameters 2, 3 and 4 mm). The angle was defined as positive if the condenser was below the evaporator in the test; an HP cannot work if the angle is greater than +45º.

As the interest in silicon HPs has increased, Hung et al. [43] reported on work on the effects of geometric design on the thermal performance of star-groove MHPs. Comparisons between the star-groove and regular polygonal MHPs were conducted and the factors contributing to the enhancement of heat transport due to the variations in geometrical parameters were identified and discussed. Ha and Peterson [46] and Sartre et al. [47] also studied triangular MHP with aluminium/ammonia. Launay et al. [26] have also used MHP arrays etched by silicon wafers in their investigations of cooling electronics. The results show that the effective thermal conductivity of the silicon wafers with an artery MHP array is significantly improved compared to massive silicon. Peterson and Ma [48] developed a detailed mathematical model for predicting the heat transport capability and temperature gradients that contribute to the overall drop in axial temperature as a function of heat transfer in an MHP.

## 3. Small two-phase loops for electronics

### *3.1. Loop heat pipes and capillary pumped loops*

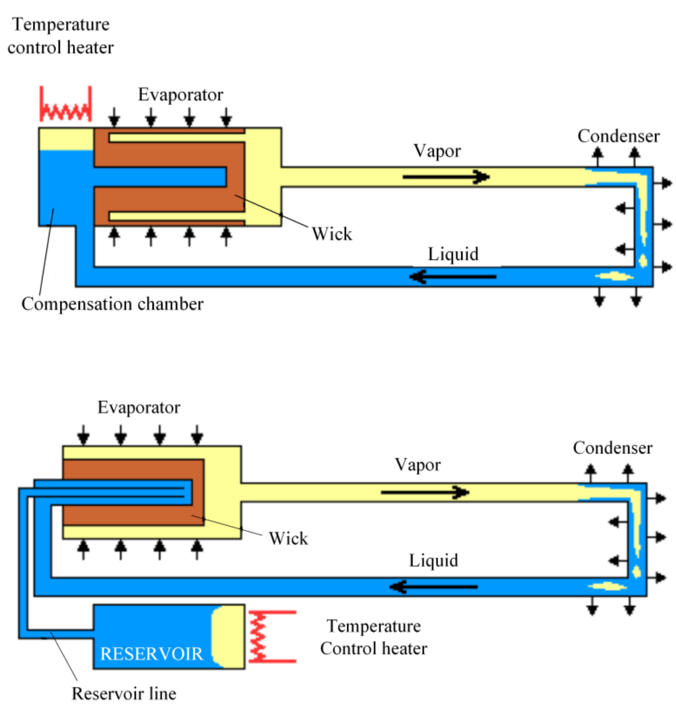


**Figure 6. Loop heat pipe and capillary pumped loop [49].**

Unlike traditional HPs, TPLs separate the tubes and wicks, which bring about enhanced ability and broader applications. The TPLs, including LHPs and CPLs, are the one of the most promising technologies for cooling electronics. The first feasibility study of CPLs was performed by Stenger in 1966 [50] and LHPs were developed and tested in 1972 in the former Soviet Union [51]. Compared to HPs, LHPs offer many advantages in terms of operation against gravity, maximum heat transport capability, smooth walled flexible transport lines, and rapid diode action [52]. An LHP is very similar to a CPL, except that the LHP has a compensation chamber (CC) instead of a remote reservoir [53, 54]. As shown in Figure 6, the basic distinction between CPLs and LHPs is clearly the position of the CC, which has a significant impact on the design and operation of the capillary loop [52]. The CC is directly connected to the evaporator, which simplifies the LHP start-up and operation vapour-tolerance. However, the CC in CPLs is separated by the connection tube, which requires preconditions. A comparison between LHPs and CPLs is shown in Table 2. Launay et al. [52] concluded that the CC can simplify the LHP start-up and make the LHP operation vapour-tolerant, which contributes to system robustness under various conditions; however, the LHP is a more complex system with strong coupled thermal and hydrodynamic characteristics between the CC and evaporator. Currently, researchers are showing intense interest in the development of LHPs/CPLs to solve heat problems in electronics and other small devices. Moreover, the liquid/gas channels that penetrate the wicks under local hot spot are becoming smaller and smaller with better cooling performance.

**Table 2. Comparison between LHP and CPL.**

| | CPL | LHP |
|---|---|---|
| Compensation chamber (CC) connected to evaporator | In direct | Direct |
| Preconditions for start-up | Yes | No |
| Primer wicks needed | Yes | No |
| Secondary wicks needed | No | Yes |
| Complexity due to thermal and hydrodynamic couples | No | Yes |
| Temperature and pressure dynamic stabilities | Poor | Good |

*3.2. Principles of loop heat pipes*

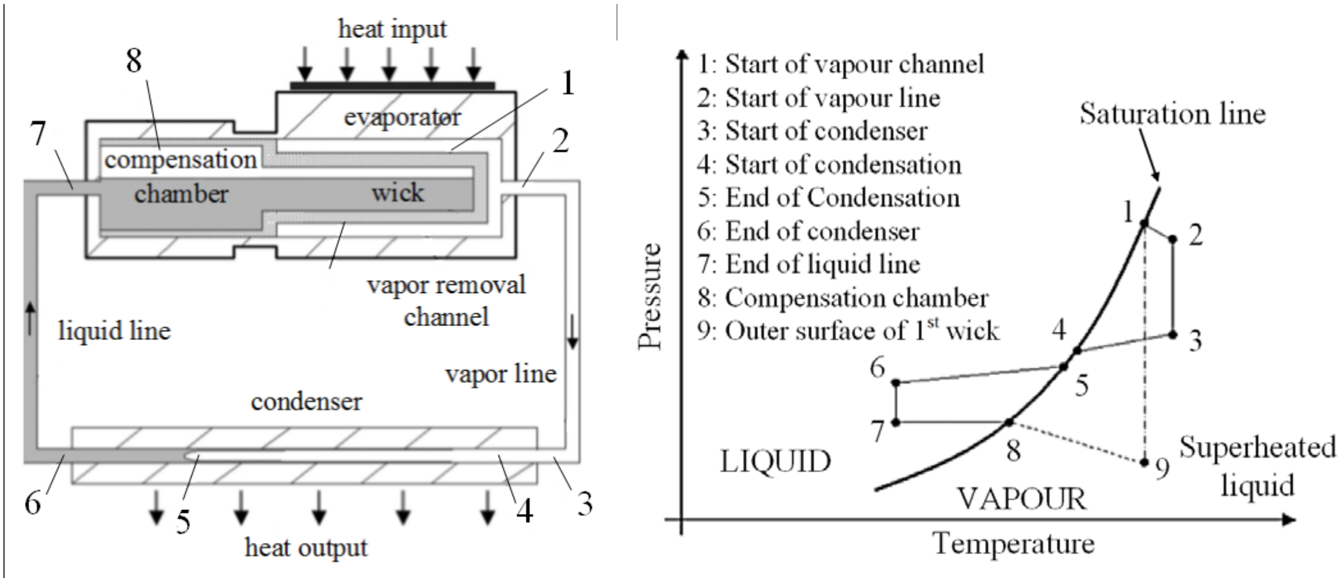


**Figure 7. Geometry of an LHP and T diagram for LHP steady-state operation (capillary controlled mode) [51, 52, 55, 56].**

The operation of an LHP is based on the same physical processes as those of conventional HPs [51, 52, 56-58]. The LHP consists of a capillary pump (also called an evaporator), a CC (also called a reservoir), a condenser, and vapour and liquid transport lines (Figure 7). Only the evaporator and the CC contain wicks; the rest of the loop can be created using smooth tubing, unlike the traditional HPs. The liquid is vaporized as a heat input $Q_e$ supplied to the evaporator, which is indicted as point 1 in the P-T diagram of Figure 7. The liquid is pumped by the capillary forces of vapour evaporator wicks from the CC. The vapour becomes superheated and its temperature increases, especially in the region that is in contact with the heated evaporator wall, but the pressure drops at the exit of the grooves (point 2). Then, the vapour moves to the vapour line with a constant temperature due to the almost thermally-isolated tube, but the pressure drops along the vapour line until it reaches the entrance to the condenser (point 3). The vapour is condensed as the temperature decreasing to its boiling point. During condensation, the vapour is cooled as the temperature and pressure decrease (point 4 to point 5). At the end of the condensation period (point 5), all of the vapour is condensed into liquid. After the condensation, the liquid is continuously cooling and begins to be subcooled inside until it reaches the end of the condenser (point 6). The heat dissipated by the condenser from point 3 to point 6 is $Q_c$. The subcooled liquid flows into the liquid line, but its temperature may increase or decrease depending on whether the liquid loses or gains heat from the ambient atmosphere. As the liquid reaches the CC inlet (point 7), the working fluid is heated by the heat conducted from evaporator to the end of the CC (point 8), which is connected to the wick. The evolution from point 8 to point 9 corresponds to the liquid flowing through the wick into the evaporation zone. On the way, the liquid may be superheated, but boiling does not take place because it remains in such a state for too short a time.

The CC is the largest component (by volume) of the loop and is often an integral part of the pump. It has two main functions[52]: (1) to accommodate excess liquid in the loop during normal operation, and (2) to supply the capillary pump wick with liquid at all times. The primary wick, which is located in the evaporator, is made of fine pores for high capillary pressure, but the secondary wick forms the connection between the evaporator and the reservoir to supply the primary wick with liquid, particularly when the reservoir is below the evaporator or under microgravity conditions. Both the liquid and vapour lines are made of small-diameter tubes that can easily be arranged around the hot devices. The operating principle of the LHP is as follows. Under steady state conditions, the liquid is vapourized and the menisci form due to the capillary forces at the liquid/vapour interface in the evaporator wick for a heat input supplied because the vapour temperature and pressure is higher in the evaporator zone (vapour grooves) than in the CC. The wick in this case serves as a "thermal lock"[51, 52]. At the same time, hotter vapour cannot penetrate the CC through the saturated wick due to the capillary forces that form the interface. Thus, another function of the wick is that of a "hydraulic lock"[51, 52]. The difference in pressure causes the displacement of the working fluid around the loop. Therefore, three two-phase interfaces may exist in the LHP simultaneously: in the evaporator zone, in the condenser and in the CC. As the heat load changes, these interfaces may shift depending except in the evaporator and the excess liquid is stored into the CC. As shown in Figure 9, Jung et al. [59] and Muraoka et al. [60] created a new type of CPL with a porous wick element in the condenser instead of the conventional tube condenser, which reduced or eliminated the start-up problem and the occurrence of pressure oscillation during operation.

*3.3. From small to micro*

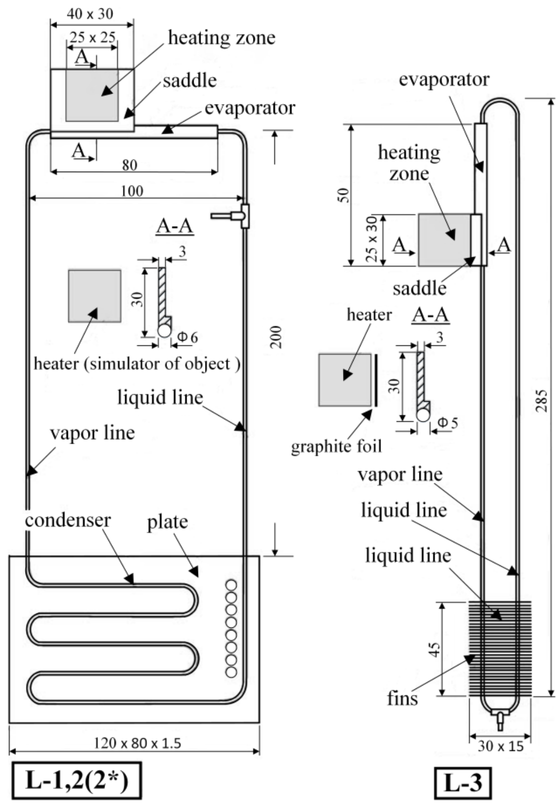


**Figure 8. Schemes of mLHPs of ‘‘L’’ type [61].**

LHPs can obtain better connections between the hot spot and heat sink due to the relatively flexible loop [62, 63]. As shown in Figure 8, Pastukhov et al. [61] developed a mini size LHP for remote heat exchanger (RHE) systems. This ‘‘L’’ loop has an effective length of approximately 250 mm and evaporators 5 and 6 mm in diameter. The working fluids ammonia and acetone ensured sufficient heat-transfer efficiency in the temperature range from 50 to 100ºC. Chen et al. [64] reported the mLHP can be used for an evaporator heat load of up to 70 W with a cylindrical evaporator of 5-mm outer diameter and 29-mm length at 75°C. Maydanik et al. [65] tested the mLHP with heat loads of 100 W to 200 W for distances of up to 300 mm in the temperature range from 50 to 100°C with ammonia and water as the working fluids. Singh et al. [66] demonstrated that the mLHP with a flat disk shaped evaporator for the thermal control of computers was capable of transferring a heat load of 70 W through a distance of up to 150 mm using 2-mm diameter transport lines.

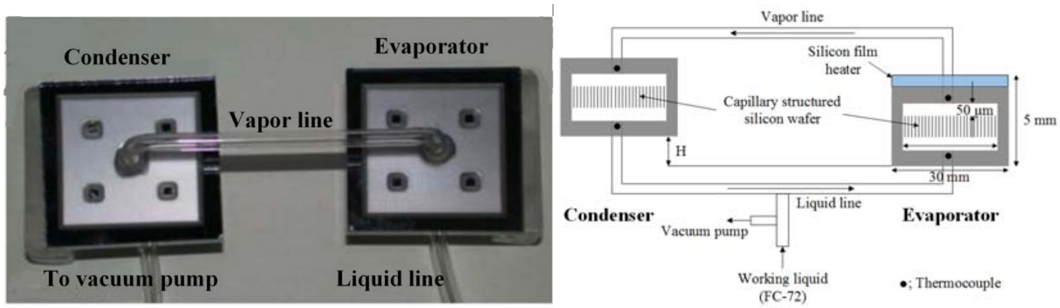


**Figure 9. A capillary-pumped loop (CPL) with microcone-shaped capillary structure [59].**

To achieve a higher heat transfer coefficient and heat transfer surface area per unit flow volume, MLHP and MCPL were created with smaller hydraulic diameters [13]; the "micro" typically indicates micro wicks. Navdeep et al. [67] recently built and tested MLHPs to demonstrate the feasibility of two phase cooling at the micro scale. Hamdan et al. [49] reported on the performance of an MLHP (100 W/cm$^2$) utilizing a coherent porous silicon wick with 5 $\mu$m effective pore diameter and porosity of 50% or higher. MCPLs were demonstrated with micro fabrication by Jung et al. [59]. Their CPL can handle a heat flux of approximately 6.22 W/cm$^2$ for the air-cooled condenser. Kirshberg et al. [68] reported that the MCPL resulted in a backside cooling effect of at least 7°C when a laser delivered 7.5 W with a spot-size diameter of 1.0 mm. Wang et al. [69] tested MCPLs that can be executed by yielding input heat fluxes of 185.2 W/cm$^2$ at an evaporator temperature of 165°C. Finally, Ghajar et al. [70] integrated the condenser, evaporator, vapour and liquid line in one process to obtain a compact LHP. A typical MEMS-based integrated CPL with a micro-cone-shaped capillary structure is shown in Figure 9. Jung et al. [59] and Muraoka et al. [60] created a new type of CPL with a porous wick element in the condenser instead of the conventional tube condenser, which reduced or eliminated the start-up problem and the occurrence of pressure oscillation during operation. It consisted of an evaporator and condenser of the same size, 30 × 30 × 5.15 mm$^3$, that were fabricated using two glass wafer layers and one silicon wafer layer. An array of 56 × 56 cone-shaped micro-holes that generates the capillary forces was fabricated and inserted above the CC for liquid transportation as micro wicks. The same cone-shaped microstructure was used in the condenser to create a stable interface between the liquid and vapour phases. With an allowable temperature of 110°C on the evaporator surfaces, the CPL can handle a heat flux of approximately 6.22 W/cm$^2$ for the air-cooled condenser.

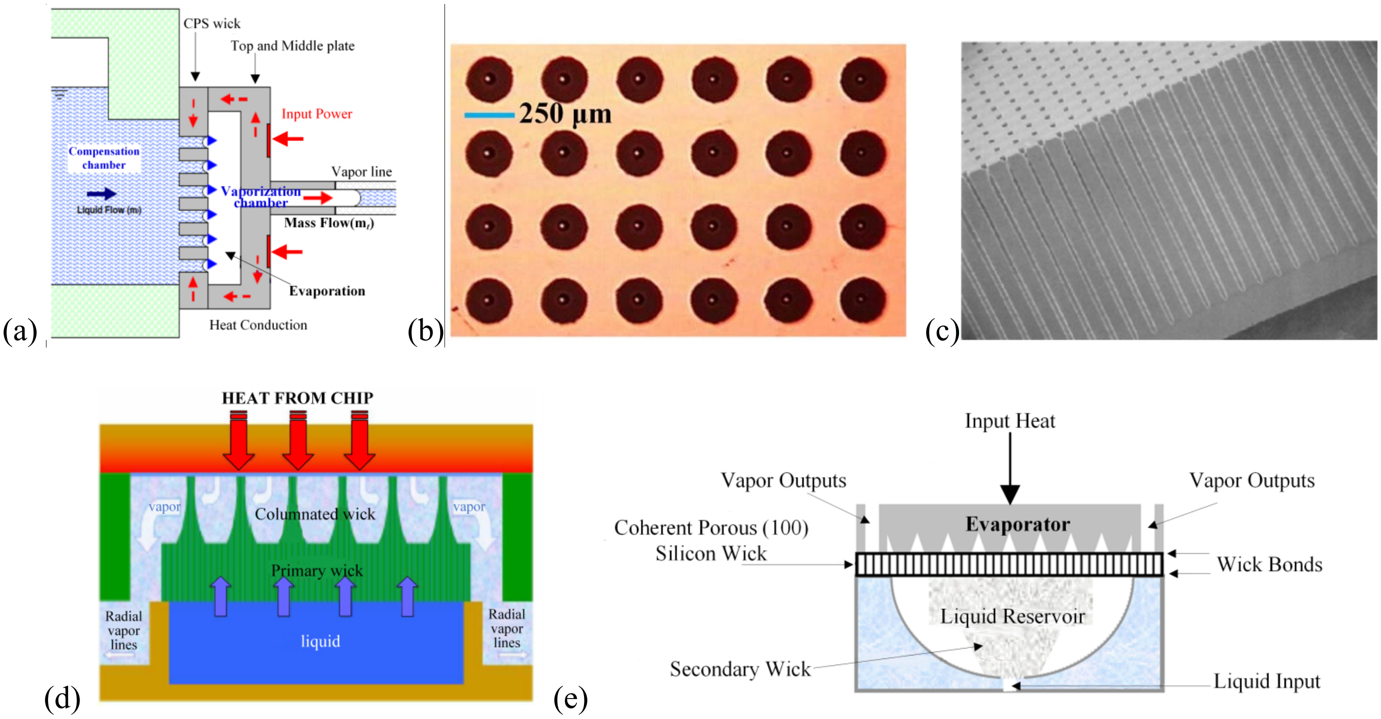


**Figure 10. (a) Heat transfer to the vaporization chamber in a MEMS bubble pump [71]; (b) Capillary array on microcapillary-structured silicon wafer in CPL [59]; (c) Coherent porous silicon (CPS) wick [72];(d) Micro-columnated CPS wicking structure [67]; (e) Silicon component of micro loop heat pipe [73].**

Because the liquid will evaporate in the evaporator with a heat input, the wick works as a “thermal lock” and “hydraulic lock”. Figure 10 (a) shows a schematic of the evaporator section when the system reaches the quasi-steady state condition, where the liquid injected from the CC is vaporized. The temperature of the working fluid is increased as heat is applied until the liquid begins to vaporize, after which all of the liquid in the vaporization chamber will gradually change into vapour. The liquid-vapour interface is formed as the menisci, which are supported by the capillary force. The interface in the vapour line is then moved to the loop side as the vapour pressure is increased. This movement continues as the vapour is cooled in the condenser.  Thus, it pumps the working fluid without any external pump.

The wick is the most important factor in driving the liquid with heat input. Meyer et al. [53] fabricated a SiC MCPL using high density interconnected processing techniques with etched trapezoidal grooves. Jung et al. [59] developed an array of 56 × 56 cone-shaped microholes 55 $\mu$m in diameter at the liquid side and 250 $\mu$m in diameter at the vapour side fabricated in the middle of a 24 × 24 $mm^2$ silicon wafer with a pitch of 430 $\mu$m, as shown in Figure 10 (b). Holke [72] produced wicks using coherent porous silicon (CPS) in silicon wafers with pore diameters ranging from 1 to 8 $\mu$m and centre-to-centre distances ranging from 4 to 10 $\mu$m. As per Dhillon et al. [67], the columnated wick can be fabricated from the primary wick using standard dry etching techniques. The secondary wicks for LHPs/CPLs are indispensable [67, 73, 74]. As shown in Figure 10 (e), Cytrynowicz et al. [73] used quartz fibre as a secondary wick to conduct the liquid to the primary wick, which provides the necessary capillary pressure to deliver water to the primary wick while maintaining a low pressure drop.

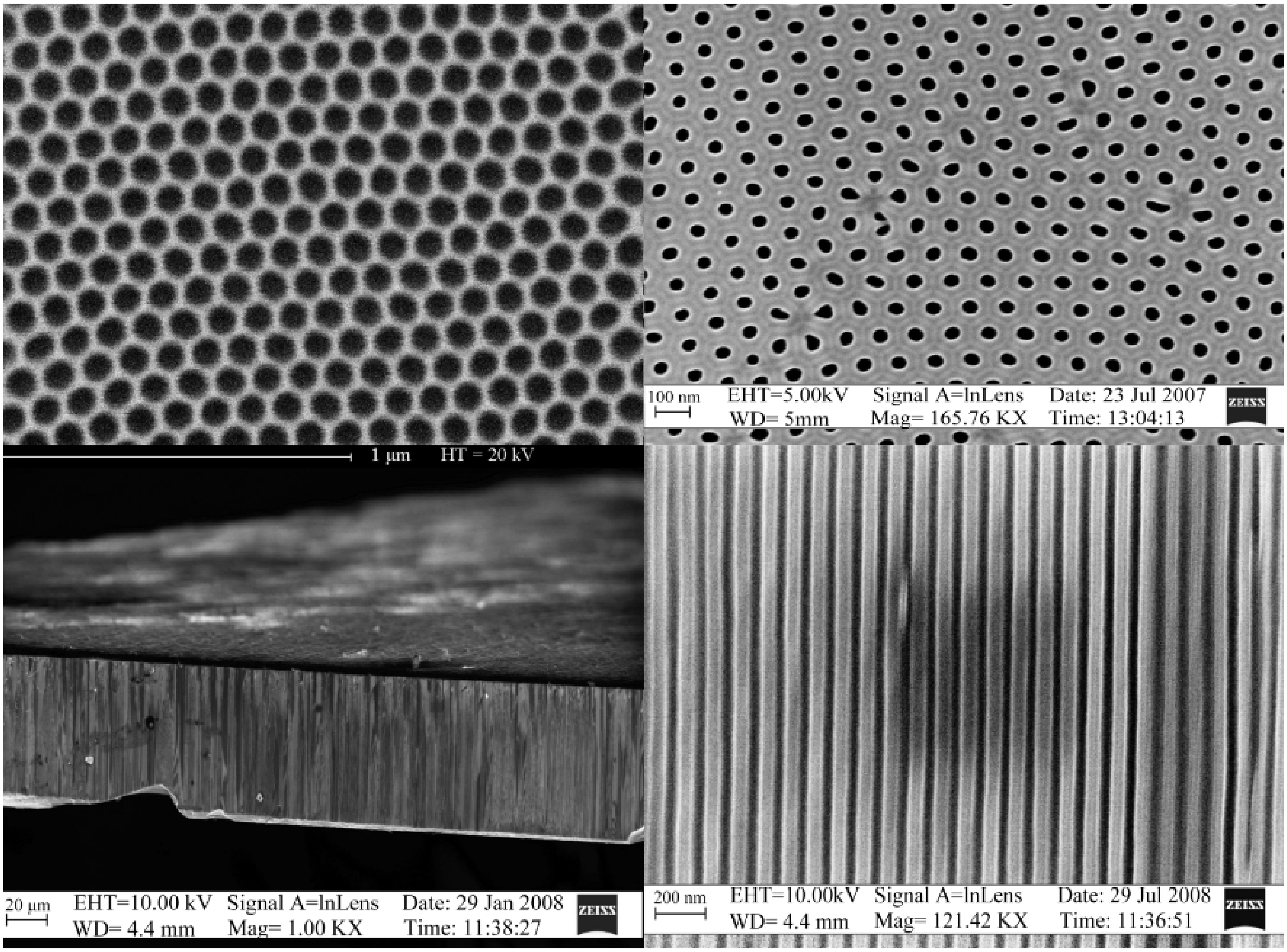


**Figure 11. SEM images showing the CNT pipe (a: top left) surface of porous alumina template prior to CVD treatment; (b: top right) template after CVD now covered in a layer of amorphous carbon that has reduced the diameter of the pores; (c: bottom left) cross section through snapped membrane; (d; bottom right) higher magnification view of cross section revealing the well-aligned and highly regular carbon nanopipe array [75, 76].**

With the boom in nano technology, especially nano carbontubes (CNT), in this century, the behaviour of fluid flowing through nanoscale channels has also been investigated [75]. The practical applications based on nanofluidic technologies in medicine and process engineering have been produced only recently [75, 77]. Majumder et al. [78] reported an average velocity through 7 nm pores in an aligned sealed array of multi-walled CNT (MWNT) of more than 60,000 times that of flowing water, approximately 32,000 times greater for ethanol and approximately 4,000 times greater for decane than the values predicted using conventional fluid flow theory. Further, Holt et al. [79] reported minimum flow enhancements in the range from 560 to 8400 for water although even smaller 1-2-nm diameter pores in an aligned array of double-walled CNT were sealed in a silicon nitride matrix. Their experiment indicated that a strong capillary force existed in the nanostructure. As calculated by the Young-Laplace equation [67, 73, 80], Figure 13 (a) shows that the millimetre of water increased dramatically with a decreasing tube diameter; however, the conventional theory may not predict the microfluidic performance at the nanostructure. A recent theoretical investigation [81-83] included a molecular dynamics (MD) study of rapid water transport in CNT. The force driving liquid through the nanotube may be much stronger than predicted. Ranjan et al. [84, 85] developed a model to calculate the evaporating liquid meniscus in wick microstructures under saturated vapour conditions. For a small diameter wire (10 $\mu$m), the percentage thin-film area of the meniscus is quite high (>80 %), and hence, the base heat flux is highest at the smallest diameter.

## 4. Small vapour chambers for electronics

### *4.1. Vapour chambers*

The VC is a special type of HP that is a particularly good heat spreader for electronics. VCs are also referred as flat HPs and were widely applied due to their uniform temperature distribution and large condensation area [86-90]. The design of VCs is similar to that of HPs. Reyes et al. [91] presented an overall analysis including an experimental and theoretical/numerical study on a vertically placed VC-based heat spreader intended for avionics applications. They considered the boiling inside, heat spreading and natural convection simultaneously. The experimental results were also used to calibrate a theoretical and numerical model of heat spreader behaviour. According to the calibrated mode, an optimization process was carried out to find the minimum weight heat spreader compatible with a series of design requirements. Koito et al. [92] studied the velocity, pressure and temperature distributions inside the vapour chamber by numerically solving the equations of continuity, momentum and energy. From the numerical results, the capillary pressure head necessary to circulate the working fluid was estimated and the temperature drop inside the vapour chamber was determined. More recently, Hassan and Harmand [93] presented a 3D transient model for VCs and the effect of nanofluids on their performance. The return of liquid from the wick region adjacent to the condenser wall to the wick region adjacent to evaporator wall was considered in the numerical model coupled with a transient hydrodynamic model. The newly developed VC for electronics is shown in Figure 12 as developed by Chang et al. **[94]**. The interior dimension of the present thin VC is 110 (length) X 50 (width) X 0.5 (height) $mm^3$ and the capillary layer is constructed using 0.05 mm deep parallel or staggered square grooves with a copper woven wire mesh sintered above the staggered grooves in the evaporator. Given the prevailing liquid/vapour phase change activities within vertical/horizontal VCs, the transmission of heat flux from the small heater area to the larger condenser cooling area is considerably improved from the copper-plate counterpart. The ratio of thermal resistance between the vertical and horizontal VCs and copper are reduced to the respective ranges of 0.571–0.951 and 0.683–0.878.

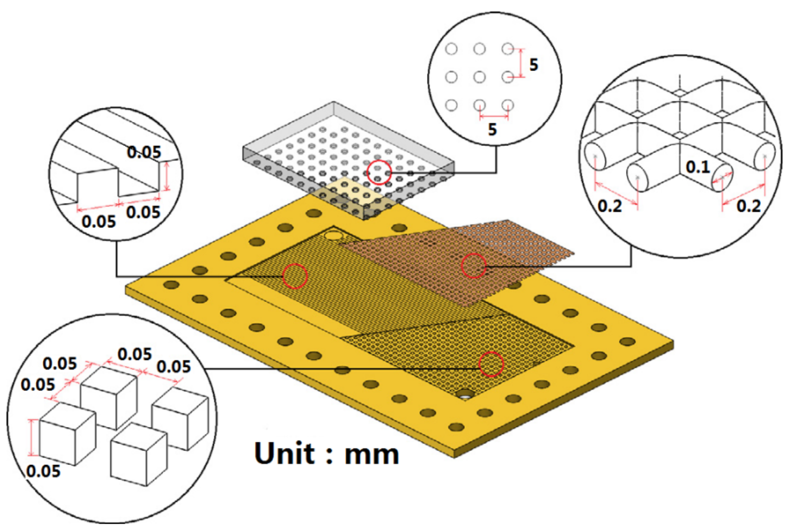


**Figure 12. Capillary structure in test VC [94].**

*4.2. Nano wicks in vapour chambers*

Although the VC or flat HP is normally used as a mini or even larger size, micro wicks, which supply capillary force, are always required [86, 87, 95]. The nano wicks made of CNT were firstly applied in VCs as a nano-tech improvement [75, 76, 96]. As shown in Figure 13 (b), Weibel et al. [96] designed integrated, nanostructured wicks for high-performance VCs. They reported that when using interspersed nanostructured wicking surfaces, the evaporator thermal resistance may be reduced significantly when adequately sized feeder wicks are utilized and the relative micro to nano wick area is optimized. They further proposed the process of combined micro and nano scale surface structuring to enhance both evaporation and boiling heat transfer from porous wick structures [97]. The CNT coating was shown to reduce the surface superheat temperature by as much as 72% by initiating boiling at low heat fluxes and avoiding the boiling incipience temperature overshoot observed for uncoated samples. Additionally, many studies and fabrications are taking place that use the CNT tube for fluids. Melechko et al. [98] reported a general method for creating patterned arrays of silica nanopipes precisely positioned over pores in a silicon nitride membrane on a silicon substrate. Bau et al. [99] described another method for constructing a nanofluidic device comprising a single carbon nanopipe (diameter 250 nm) connecting two fluid reservoirs. Flashbart et al. [100] described fabrication using contact printing of a microfluidic array with nanochannel interconnects to ensure their device could take advantage of nanocapillary effects. Han et al. [101] used surface micromachining on silicon nitride, silica and polysilicon in combination with micromoulded polydimethylsiloxane to fabricate flexible nanofluidic device architectures.

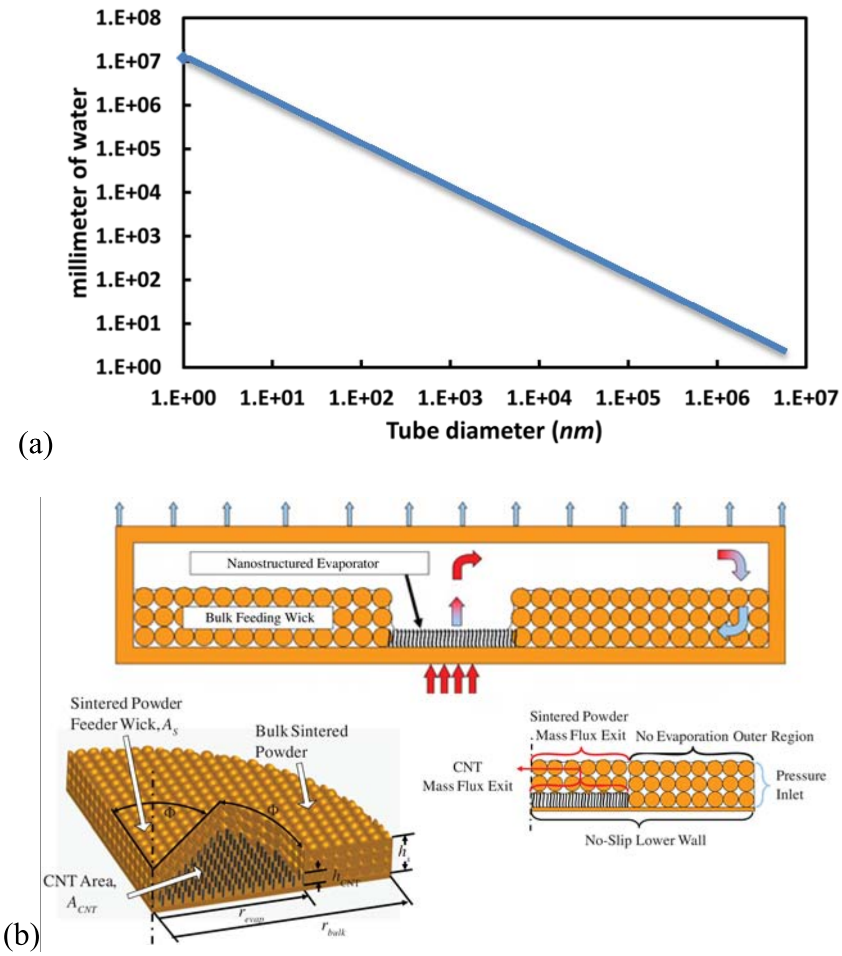


**Figure 13. (a)The millimetres of water increases with decreasing tube diameter; (b) Design of integrated nanostructured wicks for high-performance vapour chambers [96].**

## 5. Configurations and fabrication

### *5.1. Materials*

In general, both traditional HPs and MHPS are made from metals. As shown in Figure 14(a), a series of tests was performed on miniature copper-water HPs copper with diameters of 2, 3 and 4 mm by Murer et al. [45]. Sintered HPs are shown in Figure 14 (b) for porous materials produced with atomized copper powder with particle diameters ranging from 20 to 50 $\mu m$. MHPs of the curved rectangular type and curved triangular type with 1-2 mm of the equivalent diameter were fabricated by Moon et al. (Figure 14 c) [21]. The copper was used to fabricate even smaller MHPs on the central circle with a 14-mm diameter. Seventytwo rectangular grooves, each narrowed to 200 $\mu$m in width and 5.5 mm in length, are positioned in this circle, which is shown in Figure 14 (d).

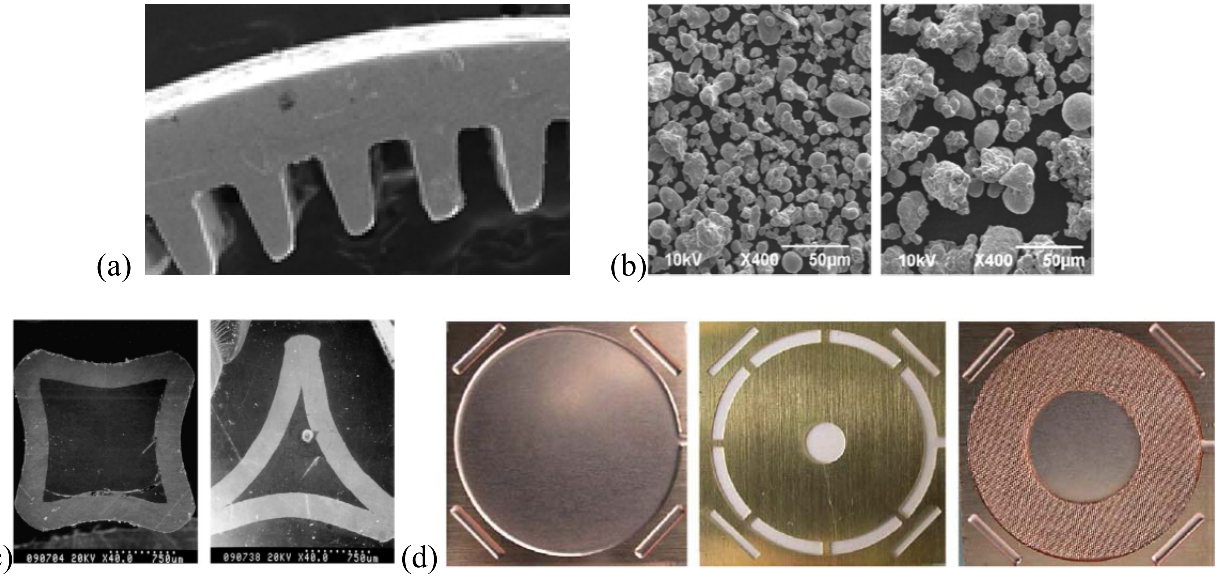


**Figure 14. Cross-section of micro-heat pipe: (a) Traditional HPs with grooves [45]; (b) Electronic microscopy image 400x on sintered porous media of HPs [23]; (c) Curved rectangular type and curved triangular type [21]; (d) The diagram showing the structure of each layer of a copper-screen-styled micro heat pipe heat spreader; Left: gas phase; central: partition panel; right: liquid phase [41].**

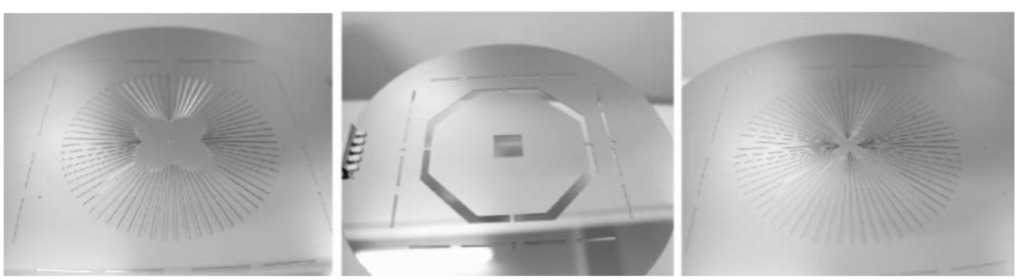

**Figure 15. Fabrication and test of radial grooved micro heat pipes [42].**

Cotter [34] introduced silicon MHPs with a hydraulic diameter of 10 to 500 $\mu$m. Many researchers investigated the MHP [17, 25, 102] as shown in Figure 1 (b) and Figure 3. An actual view of the shape of the vapour phase, liquid phase and central interface of the MHP after etching is shown in Figure 15; it is similar to the copper-screen-styled MHP. The width at the inner end of groove is 350 $\mu$m, the width at outer end of the groove is 700 $\mu$m and the etching depth is 162.5 $\mu$m. The silicon process can definitely applied to LHPs/CPLs, as shown in Figure 9 and Figure 15. Further, Dai et al. show a type of micromembrane-enhanced microchannel wick consisting of a single-layer of copper woven meshes and a silicon microchannel array in Figure 16. The superhydrophilic hybrid wick was fabricated by coating micromembrane-enhanced microchannels with 20 nm-thick silica ($SiO_2$), using the atomic layer deposited (ALD) technique. Rapid ALD $SiO_2$ coatings improve the thin film evaporation of water on hybrid wicks by up to 56%.

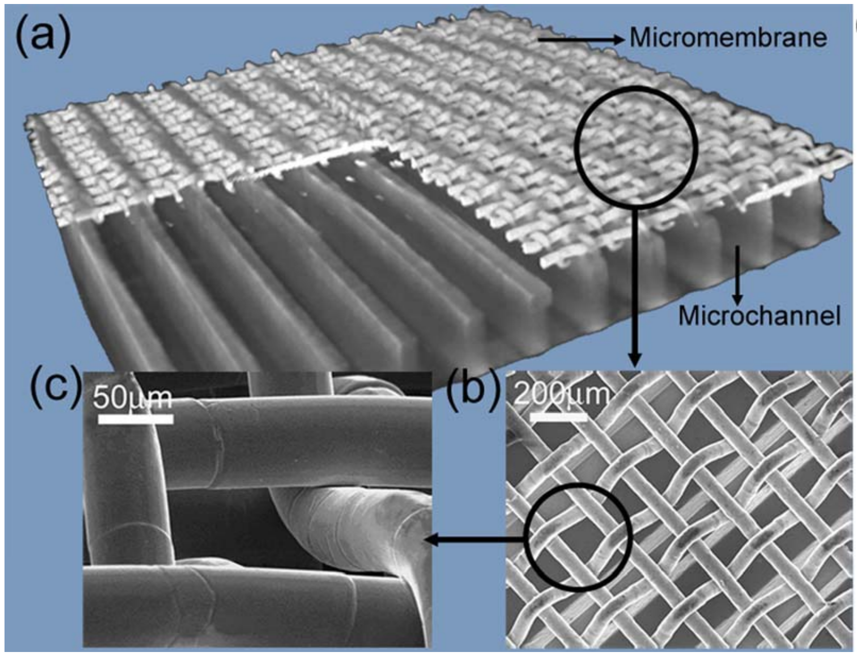


**Figure 16. Structure of the micromembrane-enhanced microchannel wicks [103, 104]**

(a) 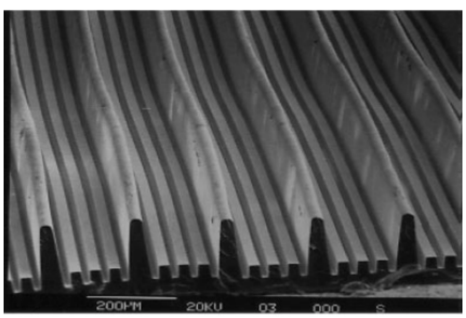 (b) 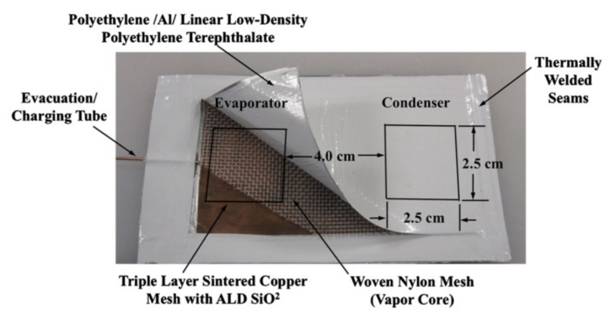


**Figure 17. (a) Flexible polymer micro heat pipes with rectangular [105, 106] and (b) Flat flexible polymer heat pipes [107].**

The metallic structure of HPs exhibits relatively high physical rigidity, as do the silicon HPs. The concept of a flexible HP initially appeared in a paper published in 1970 [108]. It has the advantage of applicability in multiple possible configurations where the heat sink may be out of plane with the heat source, allowing heat removal from oscillating heat sources. Schweickart and Buchko [109] used flexible HPs containing ammonia as the working fluid and a rolled screen mesh wick for CCD cooling in the advanced camera with flexible stainless steel for external tubing. In general, however, the HP with a flexible adiabatic section was developed with a wickless metal tube. In 2001, McDaniels and Peterson [110] presented analytical modelling and estimated the thermal conductivity of a flat, flexible, polymer HP with a grooved wicking structure to be approximately 740 W/mK. Another MHP channel design that is currently being investigated consists of flexible rectangular or trapezoidal micro channels fabricated in a polymer material with methanol and ethanol as the working fluids, as shown in Figure 17(a) [106]. The material is polypropylene and individual MHPs have an internal dimension of 200 $\mu$m with 26-$\mu$m-wide capillary grooves. More recently, Oshman et al. [111] fabricated an HP on a flexible liquid crystal polymer substrate using micro-machining techniques compatible with printed circuit board technologies. The device transferred up to 12 W of power with an effective thermal conductivity of up to 830 W/mK. As shown in Figure 17 (b), Oshman et al. [107] developed a flat, flexible, lightweight, polymer HP with the overall geometry of 130 × 70 × 1.31 mm$^3$. It was made from commercially available low-cost film composed of laminated sheets of low-density polyethylene terephthalate, aluminium and polyethylene layers. Recently, Yang et al. [112] demonstrated that a vapour chamber consists of a 1 mm thick copper frame sandwiched between the top and bottom sheets of FR4 polymer. Additionally, copper meshes were used for the wick structure inside the FR4 vapour chamber, and the thermal resistance of the substrate was reduced by 57% with thermal resistance via a cooling LED module located in the centre of the top surface.

### *5.2. Structure, fabrication and process*

Traditional HPs were made from metal, and MHPs with a diameter smaller than 2 mm can also be made from metal. Li et al. [20] (Figure 1a) created an MHP with a digitally described, mathematically modeled trapezium grooved wick that had different groove structures manufactured by high speed spinning. Their analysis showed that better heat transfer performances can be obtained in MHPs with small-angle dovetailed, rectangular and small-angle trapezoidal grooved wick structures when the groove depth is 0.2-0.3 mm and the top-width-to-depth ratio is 1.2-1.5 [22]. The collapse of thin-walled micro-grooved HPs was also analysed [40]. MHPs of the curved rectangular and curved triangular types with 1-2 mm of the equivalent diameter were fabricated by Moon et al. (Figure 14 b) [21]. Kim et al. [113] reported on experiments performed on microporous coated surfaces on flat and cylindrical heaters with micron-size aluminum particles as the microporous structures on the heated surfaces.

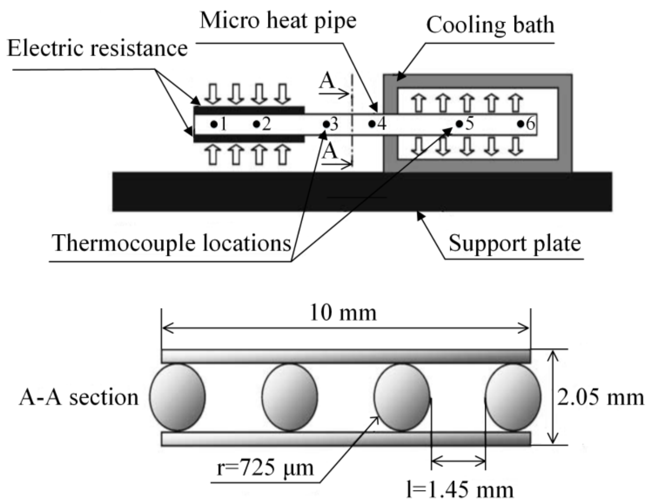


**Figure 18. Schematic view of the wire plate MHP array and thermocouple Locations [38].**

Wire plate HPs are simple, reliable simple devices that are a good alternative for grooved mini heat pipes due to the high quality of the sharp grooves, their low cost and simple fabrication process. A typical copper/water wire plate MHP was investigated by Launay et al. [38] as shown in Figure 18. The experimental results showed that its effective thermal conductivity is improved by a factor of 1.3 compared to the empty MHP array. Essentially, the process of wire plate MHP is similar to that of a flat HP [115] with a more involved manufacturing process. Wang and Peterson [37] developed the flat MHP that utilized arrays of parallel metal wires that were sandwiched between two thin metal sheets. Recently, Paiva et al. [114] dramatically enhanced the maximum heat transfer transport by groove using wire mini HPs. They reported that the wire plate mini heat pipes present more than two times higher heat transfer capacity than traditional geometries when compared of the maximum heat transfer capacity for one individual groove obtained with the present technology.

An MHP is typically a wickless, noncircular channel with a channel radius approximately the same as the characteristic radius of the liquid meniscus [31]. Silicon is preferred for generating the smallest MHPs. Launay et al. [26] developed MHPs with a triangular cross-section and liquid arteries fabricated by wet anisotropic etching with a KOH solution. Peterson et al. [102] and Ha et al. [116] fabricated MHPs using silicon wafers with an anisotropic etching process to produce triangular channels. Finally, Hung and Tio [117] performed a thermal analysis of a water-filled MHP with the triangular channels. Many studies of silicon MHPs were also performed based on the etching and bonding technology [25, 36, 42, 43, 118-123]. As shown in Figure 19 (a), the wicking process in a vaporization chamber was fabricated using silicon wafers including processes such as: oxidation and backside oxide etch; phosphorus diffusion; oxide strips, LPCVD nitride deposition or re-oxidation; photolithography; open windows in masking layer by RIE; etch pit initiation in silicon with KOH; photo-electrochemical coherent porous silicon wick etch; and backside mechanical lapping. Then, the plates were bonded together with VACSEAL to protect against leakage and baked in an oven for 1 hour at 260 °C. The process shown in Figure 19 (b) is similar but depicts the fabrication of radial grooved MHPs.

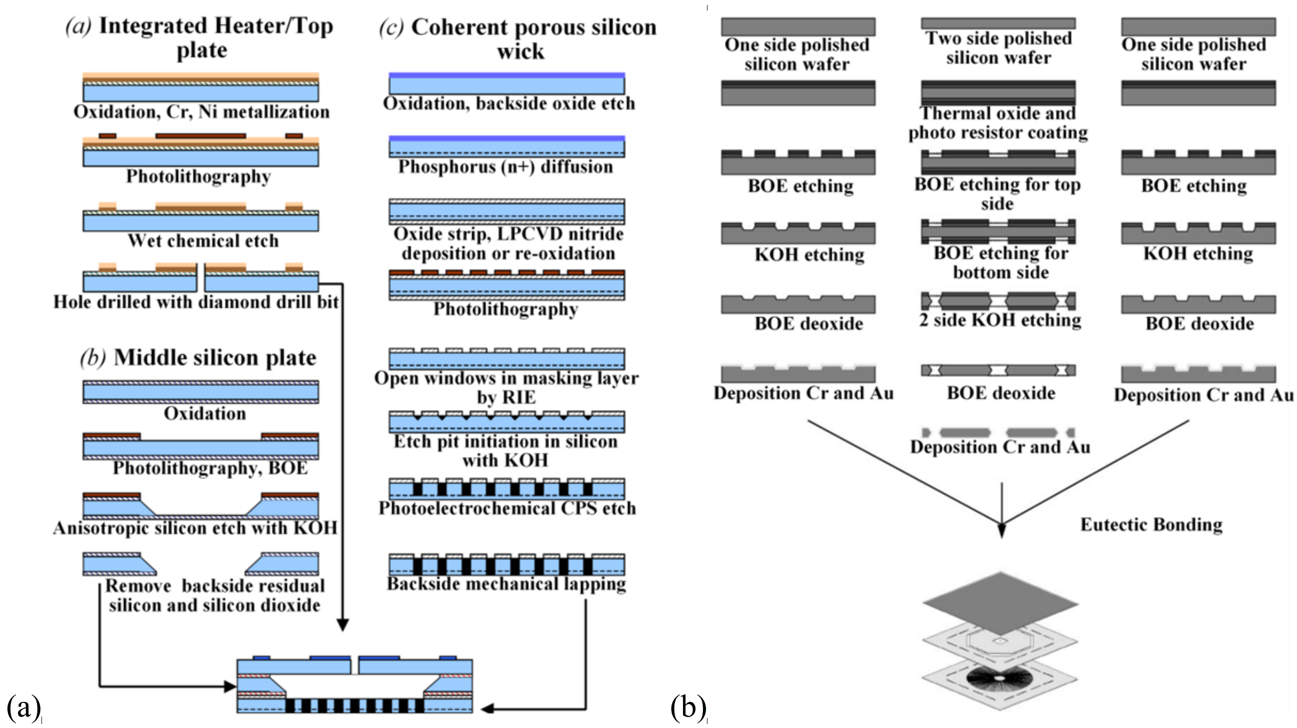


**Figure 19. (a) Processing sequence: Vaporization chamber component fabrication [71]; (b) Manufacturing flowchart of micro radial grooved heat pipe [42].**

### *5.3. Working fluids*

The working fluids of HPs are the essential components that decide the thermal performance. In general, water should be best for cooling of electronics because it has the greatest latent heat and a suitable boiling point; however, other fluid should also be seriously considered. Table 3 listed the typical physical properties of common liquids that can be considered as working fluids for HPs. Among liquid density $\rho$ (kg/m$^3$), boiling point $T_b$ (K), latent heat of evaporation $l_m$ (kJ/kg), specific heat capacity $c_p$ (J/kgK), thermal conductivity $\lambda$ (W/mK), surface tension $\sigma$ (mN/m), and dynamic viscosity $\eta$ ($p_a \cdot s$), latent heat and surface tension are the most essential parameters in HP design. Therefore, acetone, diethyl ether, ethanol, methanol, and water are the most suitable liquids. Additionally, the perfluorocarbons (FCs) and hydro-fluoro-ethers (HFEs) made by the 3 M Corporation provide this mix of properties, along with very low wetting angles on most engineering surfaces and relatively low critical pressures, thermal conductivities, and specific heats, but air solubilities approaching 50% by volume, some 25 times higher than in water [124-126].

**Table 3. Proprieties of possible working fluids for HPs to cool electronics [126-128].**

| No. | Name | $\rho$ | $T_b$ | $l_m$ | $c_p$ | $\lambda$ | $\sigma$ | $\eta$ |
|---|---|---|---|---|---|---|---|---|
| 1 | Acetic acid ($C_2H_40_2$) | 1049 | 391 | 390 | 1960 | 0.180 | 27.6 | $1.219 \times 10^{-3}$ |
| 2 | Acetone ($C_3H_60$) | 780 | 330 | 520 | 2210 | 0.161 | 23.7 | $0.324 \times 10^{-3}$ |
| 3 | Benzene ($C_6H_6$) | 879 | 353 | 400 | 1700 | 0.140 | 28.9 | $0.647 \times 10^{-3}$ |
| 4 | Bromine (Br) | 3100 | 332 | 183 | 460 | | 41.5 | $0.993 \times 10^{-3}$ |
| 5 | Carbon disulphide($CS_2$) | 1293 | 319 | 360 | 1000 | 0.144 | 32.3 | $0.375 \times 10^{-3}$ |
| 6 | Carbon tetrachloride | 1632 | 350 | 190 | 840 | 0.103 | 26.8 | $0.972 \times 10^{-3}$ |
| 7 | Chloroform ($CHC1_3$) | 1490 | 334 | 250 | 960 | 0.121 | 27.1 | $0.569 \times 10^{-3}$ |
| 8 | Ether, diethyl($C_4H_{10}O$) | 714 | 308 | 350 | 2300 | 0.127 | 17 | $0.242 \times 10^{-3}$ |
| 9 | Ethyl alcohol ($C_2H_60$) | 789 | 352 | 850 | 2500 | 0.177 | 22.3 | $1.197 \times 10^{-3}$ |
| 10 | Methyl alcohol ($CH_40$) | 791 | 337 | 1120 | 2500 | 0.201 | 22.6 | $0.594 \times 10^{-3}$ |
| 11 | Toluene ($C7H_8$) | 867 | 384 | 350 | 1670 | 0.134 | 28.4 | $0.585 \times 10^{-3}$ |
| 12 | Turpentine | 870 | 429 | 290 | 1760 | 0.136 | 27 | $1.49 \times 10^{-3}$ |
| 13 | Water ($H_2O$) | 958 | 373 | 2257 | 4217 | 0.68 | 58.9 | $0.279 \times 10^{-3}$ |
| 14 | Ammonia | 681 | 240 | 1369 | 1463.9 | | | |
| 15 | R134 | | 246 | 215 | | | 91.2 | |
| 16 | FC-40 | 1870 | 429 | 711.6 | | | 16 | $3.54 \times 10^{-3}$ |
| 17 | FC-72 | 1623 | 329 | 85.0 | 1098 | | 8.4 | $0.457 \times 10^{-3}$ |
| 18 | HFE-7100 | 1500 | 334 | 125.6 | 1180 | | 14 | $0.61 \times 10^{-3}$ |
| 19 | HFE-7200 | 1430 | 349 | 122.6 | 1210 | | 14 | $0.61 \times 10^{-3}$ |

Qu et al. [129] tested a silicon-based micro-pulsating HP with trapezoidal microchannels with a hydraulic diameter of 352 $\mu$m. FC- 72 with a latent heat of <88 kJ/kg and an average surface tension of <100 N/m, and R113 with a latent heat of 139.4 kJ/kg and an average surface tension 130.7 N/m were used as working fluids. Although the values of dynamic viscosity, latent heat, and surface tension for FC-72 were less than that of R113, which is favourable for the heat transfer of an MHP [130], R-113, which had higher $(dP/dT)_{sat}$ value, could lower the evaporator temperature. Charoensawan et al. [131] have investigated closed loop pulsating HPs with the influence characterization of varied working fluids, namely water, ethanol and R-123. They concluded that because the thermal performance is a complex combination of the above noted factors, it is difficult to prescribe or proscribe certain working fluid unless all of the boundary conditions are exactly known and individual effects have been explicitly isolated and quantified. Furthermore, Savino et al. [132] tested ordinary liquids (such as water) with the surface tension decreasing with the temperature, in which the slug moves in the direction of the temperature gradient (towards the warmer side), and a self-rewetting fluid（long-chain alcohols) with the surface tension increasing with the temperature, in which the slug is expected to move from the warmer to the cooler side. In addition, a mixture of liquids can fine-tune liquid characteristics. Savino et al. [132] mixed water, butanol, heptanol, ammonia and ethylene glycol to obtain a self-rewetting fluid. Similarly, Troniewski and Ulbrich [133, 134] changed the liquid viscosity with a varied sugarwater solution. Moreover, Miner et al. [135] reported the cooling of high-power-density micro devices with pumps using liquid metal coolants such as Hg, $Ga^{68}In^{20}Sn^{12}$, $Na^{27}K^{78}$ and SnPbInBi. The thermophysical properties of liquid metals make them attractive coolants given that their high thermal conductivity allows for efficient heat transfer and that the high electrical conductivity allows for these coolants to be pumped efficiently. Yu et al. [136] used alkali metals as working fluids in MHPs and found that they showed better evaporating characteristics for high-temperature HPs than normal working fluids.

Recently, advances in nanofabrication and processes have permitted the manufacturing of solid particles down to the nanometre scale, which has catalysed the creation of a new and rather special class of fluids termed 'nanofluids' [137]. They were successfully applied in single-phase and two-phase heat transfer devices for better heat transfer. Nguyen et al. [138] enhanced an electronic liquid cooling system using $Al_2O_3$-water nanofluid and reported that for a particular nanofluid with 6.8 % particle volume concentration, the heat transfer coefficient was found to increase as much as 40% compared to that of the base fluid and that an increase in particle concentration produced a clear decrease of the heated component temperature. Lee and Mudawar [139] studied the effectiveness of nanofluids for single-phase and two-phase heat transfer in micro-channels with water-based nanofluids containing small concentrations of $Al_2O_3$. In addition, Hassan et al. [93] analysed the effect of Cu, CuO and $Al_2O_3$ nanofluids on the vapour chamber for different wick porosities. At a volume fraction of 9% of Cu nanoparticles, which is superior to CuO and $Al_2O_3$, the maximum temperature gradient of vapour chamber decreases by approximately 19.5% for a wick porosity of 0.75 and 15.7% for a wick porosity of 0.35. Titanium nanofluids were tested by Naphon et al. [140, 141] and silver-water nanofluids were reported on by Asirvatham et al. [142] for increasing the efficiency of HPs. Yang et al. [143] carried out an experiment to study the heat transfer performance of a horizontal microgrooved HP using 0.5 wt% to 2.0 wt% 50 nm CuO nanofluid as the working fluid. In addition, Liu et al. [144] recently reported an experimental study on the heat transfer performance of a miniature thermosyphon using water-based CNT (with an average diameter of 15 nm and a length range of 5 to 15 $\mu$m) suspensions as the working fluid. Similar experiments were performed for an axially microgrooved HP using water-based CNT suspensions as the working fluid [145].

### *5.4. Limitations*

Although large quantities of heat can be removed with a small volume of coolant, a catastrophic temperature increase occurs if the power source exceeds the heat transport limitations. This work was first presented in studies of conventional HPs [146-150]. The type of limitation that restricts the operation of the HP is determined by the HP that has the lowest heat transfer rate at a specific HP working temperature (Figure 20). (1) Viscous Limit - at low temperatures, the vapour from the evaporator does not move to the condenser and the thermodynamic cycle does not occur because the difference in vapour pressure between the condenser and the evaporator may not be enough to overcome viscous forces. (2) Sonic limit - as the temperature increases, the vapour velocity continuously increases but is limited to the sonic speed, which usually occurs during HP start-up. (3) Capillary limit - the capillary pressure may be too low for the condenser to provide sufficient liquid to the evaporator, which leads to dry-out in the evaporator. Dryout prevents the thermodynamic cycle from continuing and the HP no longer functions properly. (4) Entrainment Limit - at high vapour velocities, droplets of liquid in the wick are torn from the wick and sent into the vapour, which results in dry-out. 5) Boiling Limit – dry-out occurs when the radial heat flux into the HP causes the liquid in the wick to boil and evaporate.

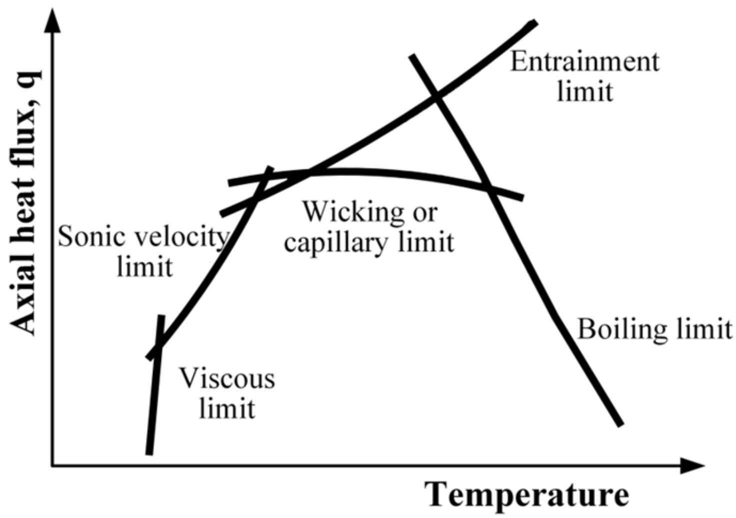


**Figure 20. Limitations to heat transport in the heat pipe[150].**

The boiling limitation also can be expressed by critical heat flux (CHF) or burnout, which is a limiting operating heat flux for the safe operation of heat dissipation applications that refers to the replacement of liquid in contact with the heated surface with a vapour blanket (Revellin and Thome [151]). The CHF is an important consideration in the design of most flow boiling systems, not just HPs. Studies have examined microchannels under saturated flow boiling conditions, coupled with an extensive database covering a wide range of fluids, channel configurations, and operating conditions. One example is that the CHF in parallel microchannels would be higher if the flow was stabilized by an orifice at the entrance of each channel. The nature of CHF in microchannels is thus different than anticipated, but recent advances in microelectronic fabrication may make it possible to realize higher power levels (Bergles and Kandlikar [152]).

## 6. Summary and discussion

The design factors of HPs used for cooling electronics are complex, ranging from structure, materials and working fluids to gravity and wicks. The development of MHPs or LHPs that enable rapid cooling for hot spots could have a significant impact for all electronic devices. Generally, the principle of design is shown in Figure 21. The dimensions can be the first parameter to be considered, namely, 1) the heat source dimension, and 2) the heat sink dimension. For instance, if the device has allowed for a large heat sink, HPs are unnecessary. Further, the dimension of the entire system will decide whether an HP, VC or flat HP is needed. The latter requires a relatively large contact surface, and similarly, traditional tubular HPs and variable conductance HPs need a relatively large space to be set up. In contrast, semiconductor chips are too small to be used with normal HPs. Secondly, the effect of wicks and gravity are emerging in tandem. Thermal diodes and pulsating LHPs cannot work without gravity and gravity has a negative effect on tubular HPs. Both MHPs and LHPs, however, can obtain special properties to transfer heat over distances of up to several meters at any orientation in the gravity field, although that ability is based on the wick position, dimension, material and structure. Therefore, the type of HP can be decided accordingly. Depending on the application, the material, wick (microgroove), structure and process will be considered next. For a semiconductor device, silicon may be favoured due to its matched CTE and standard process. For those devices requiring flexibility, polymer HP may be the best candidate due to its fast fabrication and easily application. However, HP design also requires considering the wick porosity, pipe diameter, condenser and evaporator. Last but not the least, although the calculation or simulation can provide indications of performance, experimental testing of HPs is essentially compulsory.

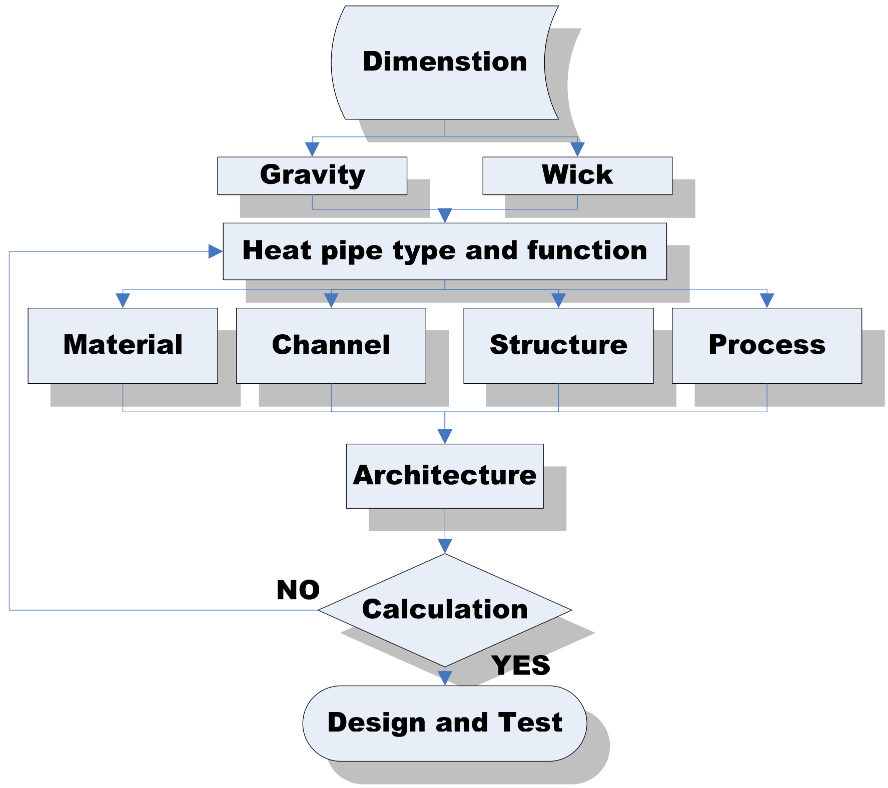


**Figure 21. Principles in the design and fabrication of HPs for cooling electronics.**

Whether MHPs or LHPs are selected for any given project, the design process does not end at the decision point. Although calculations or simulations can provide a qualitative analysis, the design of HPs depends on experimentation. Sobhan et al. [105] reported that experiments undertaken over the last two decades have examined cross-sectional shape, operating temperature, heat input, cross-sectional area of a channel, heat transfer coefficient, temperature drop, dimension and thermal resistance. The discussions and data presented in these papers were expected to act as guidelines in designing MHPs and introducing innovative designs for various applications. To aid in this endeavour, Bai et al. [153] presented a design flowchart for LHP models. This work was based on steady-state mathematical modelling. To improve solution accuracy, the liquid and vapour lines are divided into several nodes, each of which represents a certain control volume, and the calculations are conducted on every node. Further, Zhang et al. [154] have demonstrated the design, fabrication and testing of LHPs for a specific application (a solar photovoltaic/loop-heat-pipe (PV/LHP) heat pump system). Dedicated thermo-fluid and energy balance analyses were performed using computer models to calculate the operational parameters, optimize the geometrical configurations and sizes, and recommend the appropriate operational condition, after which experimental verification and modifications were applied accordingly.

## 7. Prospective and conclusion

The combined need for digital and non-digital functionalities in an integrated system is translated as a dual trend in the International Technology Roadmap for Semiconductors: miniaturization of the digital functions ("More Moore") and functional diversification ("More-than-Moore")[155, 156], which in this work is called advanced electronics. The more functions are built in, however, the more power is required; similarly, greater miniaturization leads to more concentrated power. Waste heat then creates a very high temperature hot spot accordingly. Thermal management will continue to be one of most important issues for electronics. Cooling devices are indispensable, although they are not always desirable as they usually introduce problems of large volume, overweight, hinder, and reliability. As shown in Figure 22, the advanced electronics define the device through three criteria: functionality, flexibility and reliability. (1) Functionality - more functions require more power or power density because more devices have been added to 1 $cm^3$. (2) Flexibility - this requires that all of the functional devices can be flexibly arranged anywhere the designer needs them. (3) Reliability - products should be stable, environmentally friendly and have a sufficiently long life span. Accordingly, thermal management must provide sufficient support to these criteria.

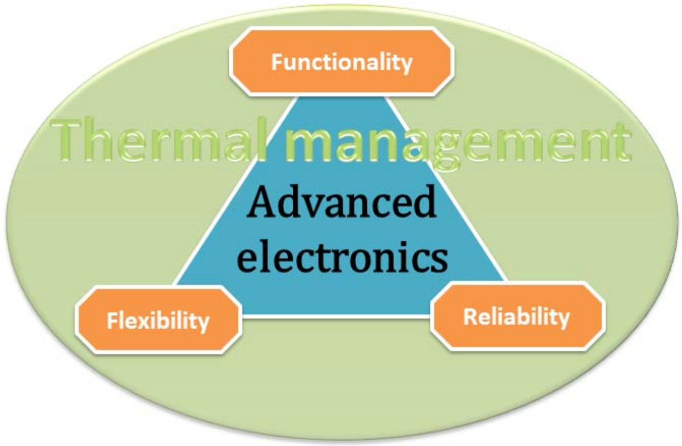


**Figure 22. Thermal management/cooling for advanced electronics**

MHPs are highly efficient heat-transfer devices for cooling electronics, especially with regard to silicon compatible processes, and although they lack flexibility, MHPs are one of the best thermal management devices for advanced electronics. Alternately, LHPs with mini/micro wicks can be used to create ramified, reversible, controllable systems for heat-transfer when mechanical flexibility and high adaptability to various operating conditions are required. The LHP process can be derived from conventional metallic HPs, silicon MHPs or polymers. CNT has become the next promising candidate for nano wicks with their outstanding nanofludic characteristics. With systematically designs based on their ultimate applications, a new generation of MHPs or MLHPs can be developed to solve the cooling problem of electronics and obtain energy recovery in recent future.

## Acknowledgments

The research is co-supported by the National High Technology Research and Development Program of China (863 Program) (Project no. 2015AA033304), the National Natural Science Foundation of China (Project no. 51303033, 61434001), the Natural Science Foundation of Guangxi Province (Project no. 2014GXNSFCB118004), the China Postdoctoral Science Foundation (Project no. 2014M550065) and Guangxi Universities Scientific Foundation (Project no. YB2014116).

## References

[1] A. Bar-Cohen, P. Wang, E. Rahim, Thermal management of high heat flux nanoelectronic chips, Microgravity Science and Technology, 19 (2007) 48-52.
[2] S.V. Garimella, A.S. Fleischer, J.Y. Murthy, A. Keshavarzi, R. Prasher, C. Patel, S.H. Bhavnani, R. Venkatasubramanian, R. Mahajan, Y. Joshi, Thermal challenges in next-generation electronic systems, IEEE Transactions on Components and Packaging Technologies, 31 (2008) 801-815.
[3] G.F. Russell, Uniform surface temperature heat pipe and method of using the same, in, Google Patents, 1982.
[4] G.J. Sheu, F.S. Hwu, S.H. Tu, W.T. Chen, J.Y. Chang, J.C. Chen, The heat dissipation performance of LED applied a MHP, in: Proceedings of SPIE, Vol. 5941, 2005, pp. 199-206.
[5] L. Kim, J.H. Choi, S.H. Jang, M.W. Shin, Thermal analysis of LED array system with heat pipe, Thermochimica Acta, 455 (2007) 21-25.
[6] Z. Lin, S. Wang, J. Huo, Y. Hu, J. Chen, W. Zhang, E. Lee, Heat transfer characteristics and LED heat sink application of aluminum plate oscillating heat pipes, Applied Thermal Engineering, 31 (2011) 2221-2229.
[7] J.B. Marcinichen, J.R. Thome, B. Michel, Cooling of microprocessors with micro-evaporation: A novel two-phase cooling cycle, International Journal of Refrigeration, 33 (2010) 1264-1276.
[8] J.B. Marcinichen, J.A. Olivier, N. Lamaison, J.R. Thome, Advances in Electronics Cooling, Heat Transfer Engineering, 34 (2013) 434-446.
[9] S.S.J. Mehendale, A. M.;Shah, R. K., Fluid Flow and Heat Transfer at Micro- and Meso-Scales with Application to Heat Exchanger Design, Applied Mechanics Reviews, 53 (2000) 175-193.
[10] S.G. Kandlikar, Two-phase flow patterns, pressure drop, and heat transfer during boiling in minichannel flow passages of compact evaporators, Heat Transfer Engineering, 23 (2002) 5-23.
[11] L. Chen, Y. Tian, T. Karayiannis, The effect of tube diameter on vertical two-phase flow regimes in small tubes, International Journal of Heat and Mass Transfer, 49 (2006) 4220-4230.
[12] J.R. Thome, Boiling in microchannels: a review of experiment and theory, International Journal of Heat and Fluid Flow, 25 (2004) 128-139.
[13] L. Vasiliev, Micro and miniature heat pipes–Electronic component coolers, Applied Thermal Engineering, 28 (2008) 266-273.
[14] F. Andros, B. Sammakia, Thermal management in electronic packaging, in, New York: McGraw-Hill Inc, 1989, pp. 154-155.
[15] L. Waller, An old idea may solve VHSIC cooling problem, Electronics, (1985) 19-20.
[16] A.D. Kraus, A. Bar-Cohen, Thermal analysis and control of electronic equipment, Washington, DC, Hemisphere Publishing Corp., 1983, 633 p., 1 (1983).
[17] H.N. Chaudhry, B.R. Hughes, S.A. Ghani, A review of heat pipe systems for heat recovery and renewable energy applications, Renewable and Sustainable Energy Reviews, 16 (2012) 2249-2259.
[18] W. Srimuang, P. Amatachaya, A review of the applications of heat pipe heat exchangers for heat recovery, Renewable and Sustainable Energy Reviews, 16 (2012) 4303-4315.
[19] M. North, C. Avedisian, Heat pipes for cooling high flux/high power semiconductor chips, Journal of Electronic Packaging, 115 (1993) 112.
[20] L. Xibing, L. Xianli, S. Zhimin, J. Hui, L. XiaoZhong, W. Shigang, H. Gang, P. Yongge, Heat Transfer Performance of Micro Heat Pipe with Trapezium-grooved Wick, in: Fifth International Conference on Intelligent Computation Technology and Automation (ICICTA), 2012, pp. 614-618.
[21] S.H. Moon, G. Hwang, S.C. Ko, Y.T. Kim, Experimental study on the thermal performance of micro-heat pipe with cross-section of polygon, Microelectronics Reliability, 44 (2004) 315-321.
[22] X.B. Li, Z. Shi, S. Wang, Q. Hu, L. Bao, H. Zhang, Analysis of structural parameters of grooved-wicksin micro heat pipes based on capillary limits, Key Engineering Materials, 499 (2012) 21-26.
[23] J.P.M. Florez, M.B. Mantelli, G.G. Nuernberg, Effective thermal conductivity of sintered porous media: Model and experimental validation, International Journal of Heat and Mass Transfer, 66 (2013) 868-878.
[24] J.P.M. Florez, M.B. Mantelli, G.G. Nuernberg, F.H. Milanez, Powder geometry based models for sintered media porosity and effective thermal conductivity, Journal of Thermophysics and Heat Transfer, 28 (2014) 507-517.
[25] M. Le Berre, S. Launay, V. Sartre, M. Lallemand, Fabrication and experimental investigation of silicon micro heat pipes for cooling electronics, Journal of Micromechanics and Microengineering, 13 (2003) 436.
[26] S. Launay, V. Sartre, M. Lallemand, Experimental study on silicon micro-heat pipe arrays, Applied Thermal Engineering, 24 (2004) 233-243.
[27] A. Mallik, G. Peterson, M. Weichold, On the use of micro heat pipes as an integral part of semiconductor devices, Journal of Electronic Packaging, 114 (1992) 436-442.
[28] G. Peterson, Overview of micro heat pipe research and development, Applied Mechanics Reviews, 45 (1992).
[29] R.J. McGlen, R. Jachuck, S. Lin, Integrated thermal management techniques for high power electronic devices, Applied Thermal Engineering, 24 (2004) 1143-1156.

[30] M. Lallemand, F. Lefevre, Micro/mini heat pipes for the cooling of electronic devices, in: 13th International Heat Pipe Conference, Shanghai, China, 2004, pp. 12-23.
[31] B. Babin, G. Peterson, D. Wu, Steady-state modeling and testing of a micro heat pipe, Journal of Heat Transfer, 112 (1990).
[32] D. Khrustalev, A. Faghri, Thermal analysis of a micro heat pipe, Journal of Heat Transfer, 116 (1994) 189-198.
[33] G. Peterson, Modeling, fabrication, and testing of micro heat pipes: an update, Applied Mechanics Reviews, 49 (1996).
[34] T. Cotter, Principles and prospects for micro heat pipes, in, Los Alamos National Lab., NM (USA), 1984.
[35] C.Y. Wang, M. Groll, S. Rösler, C.J. Tu, Porous medium model for two-phase flow in mini channels with applications to micro heat pipes, Heat Recovery Systems and CHP, 14 (1994) 377-389.
[36] M. Rahmat, P. Hubert, Two-phase simulations of micro heat pipes, Computers & Fluids, 39 (2010) 451-460.
[37] Y. Wang, G. Peterson, Analysis of wire-bonded micro heat pipe arrays, Journal of Thermophysics and Heat Transfer, 16 (2002) 346-355.
[38] S. Launay, V. Sartre, M.B. Mantelli, K.V. de Paiva, M. Lallemand, Investigation of a wire plate micro heat pipe array, International Journal of Thermal Sciences, 43 (2004) 499-507.
[39] Y. Wang, G. Peterson, Optimization of micro heat pipe radiators in a radiation environment, Journal of Thermophysics and Heat Transfer, 16 (2002) 537-546.
[40] Y. LI, T. HE, Z. ZENG, Analysis of Collapse in Flattening a Microgrooved Heat Pipe by Lateral Compression, Chinese Journal of Mechanical Engineering, 25 (2012).
[41] S.W. Kang, S.H. Tsai, M.H. Ko, Metallic micro heat pipe heat spreader fabrication, Applied Thermal Engineering, 24 (2004) 299-309.
[42] S.W. Kang, S.H. Tsai, H.C. Chen, Fabrication and test of radial grooved micro heat pipes, Applied Thermal Engineering, 22 (2002) 1559-1568.
[43] Y.M. Hung, Q.b. Seng, Effects of geometric design on thermal performance of star-groove micro-heat pipes, International Journal of Heat and Mass Transfer, 54 (2011) 1198-1209.
[44] X. Li, J. Wang, Q. Hu, L. Bao, H. Zhang, C. Wang, Capillary Limit of Micro Heat Pipe with Compound Structure of a Sintered Wick on Trapezium-grooved Substrate, Przegląd Elektrotechniczny, (2012).
[45] S. Murer, P. Lybaert, L. Gleton, A. Sturbois, Experimental and numerical analysis of the transient response of a miniature heat pipe, Applied Thermal Engineering, 25 (2005) 2566-2577.
[46] J. Ha, G. Peterson, The heat transport capacity of micro heat pipes, Journal of Heat Transfer, 120 (1998) 1064-1071.
[47] V. Sartre, M.C. Zaghdoudi, M. Lallemand, Effect of interfacial phenomena on evaporative heat transfer in micro heat pipes, International Journal of Thermal Sciences, 39 (2000) 498-504.
[48] G. Peterson, H. Ma, Temperature response of heat transport in a micro heat pipe, Journal of Heat Transfer, 121 (1999) 438-445.
[49] M.O. Hamdan, Loop Heat Pipe (LHP) Modeling and Development by Utilizing Coherent Porous Silicion (CPS) Wicks, PhD thesis, University of Cincinnati, 2003.
[50] F.J. Stenger, Experimental feasibility study of water-filled capillary-pumped heat transfer loops, NASA TM-X-1310, (1966).
[51] Y.F. Maydanik, Loop heat pipes, Applied Thermal Engineering, 25 (2005) 635-657.
[52] S. Launay, V. Sartre, J. Bonjour, Parametric analysis of loop heat pipe operation: a literature review, International Journal of Thermal Sciences, 46 (2007) 621-636.
[53] L. Meyer, S. Dasgupta, D. Shaddock, J. Tucker, R. Fillion, P. Bronecke, L. Yorinks, P. Kraft, A silicon-carbide micro-capillary pumped loop for cooling high power devices, in: Semiconductor Thermal Measurement and Management Symposium, 2003, pp. 364-368.
[54] M. Nikitkin, B. Cullimore, CPL and LHP technologies: What are the differences, what are the similarities?, in: International Conference On Environmental Systems, Danvers, 1998, pp. 10.
[55] P.Y.A. Chuang, An improved steady-state model of loop heat pipes based on experimental and theoretical analyses, PhD Thesis in the Pennsylvania State University, 2003.
[56] J. Ku, Operating characteristics of loop heat pipes, SAE transactions, 108 (1999) 503-519.
[57] S. Van Oost, B. Mullender, G. Bekaert, J.C. Legros, Secondary wick operation principle and performance mapping in LHP and FLHP evaporators, in: AIP conference proceedings, Vol. 608, 2002, pp. 94.
[58] T.T. Hoang, J. Ku, Heat and mass transfer in loop heat pipes, in: ASME proceedings, 2003.
[59] J.Y. Jung, H.S. Oh, D.K. Lee, K.B. Choi, S.K. Dong, H.Y. Kwak, A capillary-pumped loop (CPL) with microcone-shaped capillary structure for cooling electronic devices, Journal of Micromechanics and Microengineering, 18 (2008) 017002.
[60] I. Muraoka, F. Ramos, V. Vlassov, Experimental and theoretical investigation of a capillary pumped loop with a porous element in the condenser, International Communications in Heat and Mass Transfer, 25 (1998) 1085-1094.
[61] V. Pastukhov, Y.F. Maidanik, C. Vershinin, M. Korukov, Miniature loop heat pipes for electronics cooling, Applied Thermal Engineering, 23 (2003) 1125-1135.
[62] A.A. Adoni, A. Ambirajan, V. Jasvanath, D. Kumar, P. Dutta, Theoretical Studies of Hard Filling in Loop Heat Pipes, Journal of Thermophysics and Heat Transfer, 24 (2010) 173-183.
[63] A. Ambirajan, A.A. Adoni, J.S. Vaidya, A.A. Rajendran, D. Kumar, P. Dutta, Loop Heat Pipes: A Review of Fundamentals, Operation, and Design, Heat Transfer Engineering, 33 (2012) 387-405.

[64] Y. Chen, M. Groll, R. Mertz, Y.F. Maydanik, S. Vershinin, Steady-state and transient performance of a miniature loop heat pipe, International Journal of Thermal Sciences, 45 (2006) 1084-1090.
[65] Y.F. Maydanik, S.V. Vershinin, M.A. Korukov, J.M. Ochterbeck, Miniature loop heat pipes-a promising means for cooling electronics, IEEE Transactions on Components and Packaging Technologies, 28 (2005) 290-296.
[66] R. Singh, A. Akbarzadeh, C. Dixon, M. Mochizuki, R.R. Riehl, Miniature loop heat pipe with flat evaporator for cooling computer CPU, Transactions onComponents and Packaging Technologies, 30 (2007) 42-49.
[67] N.S. Dhillon, A.P. Pisano, C. Hogue, M.A. Hopcroft, MLHP–A high heat flux localized cooling technology for electronic substrates, in: ASME Conference Proceedings, 2008, pp. 621-630.
[68] J. Kirshberg, K. Yerkes, D. Trebotich, D. Liepmann, Cooling effect of a mems based micro capillary pumped loop for chip-level temperature control, in: ASME International Mechanical Engineering Congress and Exposition, 2000, pp. 1-8.
[69] C.T. Wang, T.S. Leu, T.M. Lai, Micro capillary pumped loop system for a cooling high power device, Experimental Thermal and Fluid Science, 32 (2008) 1090-1095.
[70] M. Ghajar, J. Darabi, N. Crews Jr, A hybrid CFD-mathematical model for simulation of a MEMS loop heat pipe for electronics cooling applications, Journal of Micromechanics and Microengineering, 15 (2005) 313.
[71] J. Suh, D. Cytrynowicz, F.M. Gerner, H.T. Henderson, A MEMS bubble pump for an electronic cooling device, Journal of Micromechanics and Microengineering, 20 (2010) 125025.
[72] A.D. Holke, Development of silicon chemical wet etching toward the realization of an integrated thermal-electronic package, PhD Dissertation in University of Cincinnati, 1999.
[73] D. Cytrynowicz, M. Hamdan, P. Medis, A. Shuja, H.T. Henderson, F.M. Gerner, E. Golliher, MEMS loop heat pipe based on coherent porous silicon technology, in: AIP Conference Proceedings, Vol. 608, 2002, pp. 220-232.
[74] K. Pettigrew, J. Kirshberg, K. Yerkes, D. Trebotich, D. Liepmann, Performance of a MEMS based micro capillary pumped loop for chip-level temperature control, in: 14th IEEE International Conference on Micro Electro Mechanical Systems 2001, pp. 427-430.
[75] M. Whitby, N. Quirke, Fluid flow in carbon nanotubes and nanopipes, Nature Nanotechnology, 2 (2007) 87-94.
[76] H. Masuda, K. Fukuda, Ordered metal nanohole arrays made by a two-step, Science, 268 (1995) 1466-1468.
[77] B.J. Hinds, N. Chopra, T. Rantell, R. Andrews, V. Gavalas, L.G. Bachas, Aligned multiwalled carbon nanotube membranes, Science, 303 (2004) 62-65.
[78] M. Majumder, N. Chopra, R. Andrews, B.J. Hinds, Nanoscale hydrodynamics: Enhanced flow in carbon nanotubes, Nature, 438 (2005) 44-44.
[79] J.K. Holt, H.G. Park, Y. Wang, M. Stadermann, A.B. Artyukhin, C.P. Grigoropoulos, A. Noy, O. Bakajin, Fast mass transport through sub-2-nanometer carbon nanotubes, Science, 312 (2006) 1034-1037.
[80] R. C. So, T. Gatski, T. Sommer, J. Dickey, G. Peterson, Experimental and analytical investigation of a capillary pumped loop, Journal of Thermophysics and Heat Transfer, 8 (1994) 602-607.
[81] S. Joseph, N. Aluru, Why are carbon nanotubes fast transporters of water?, Nano Letters, 8 (2008) 452-458.
[82] Q.L. Zhang, W.Z. Jiang, J. Liu, R.D. Miao, N. Sheng, Water Transport through Carbon Nanotubes with the Radial Breathing Mode, Physical Review Letters, 110 (2013) 254501.
[83] S.K. Kannam, B. Todd, J. Hansen, P.J. Daivis, How fast does water flow in carbon nanotubes?, The Journal of chemical physics, 138 (2013) 094701.
[84] R. Ranjan, J.Y. Murthy, S.V. Garimella, A microscale model for thin-film evaporation in capillary wick structures, International Journal of Heat and Mass Transfer, 54 (2011) 169-179.
[85] R. Ranjan, J.Y. Murthy, S. Garimella, Analysis of the wicking and thin-film evaporation characteristics of microstructures, (2009).
[86] S.C. Wong, K.C. Hsieh, J.D. Wu, W.L. Han, A novel vapor chamber and its performance, International Journal of Heat and Mass Transfer, 53 (2010) 2377-2384.
[87] Y. Peng, W. Liu, N. Wang, Y. Tian, X. Chen, A novel wick structure of vapor chamber based on the fractal architecture of leaf vein, International Journal of Heat and Mass Transfer, 63 (2013) 120-133.
[88] X. Ji, J. Xu, A.M. Abanda, Q. Xue, A vapor chamber using extended condenser concept for ultra-high heat flux and large heater area, International Journal of Heat and Mass Transfer, 55 (2012) 4908-4913.
[89] P. Naphon, S. Wongwises, S. Wiriyasart, Application of two-phase vapor chamber technique for hard disk drive cooling of PCs, International Communications in Heat and Mass Transfer, (2012).
[90] J.C. Wang, R.T. Wang, T.L. Chang, D.S. Hwang, Development of 30Watt high-power LEDs vapor chamber-based plate, International Journal of Heat and Mass Transfer, 53 (2010) 3990-4001.
[91] M. Reyes, D. Alonso, J. Arias, A. Velazquez, Experimental and theoretical study of a vapour chamber based heat spreader for avionics applications, Applied Thermal Engineering, 37 (2012) 51-59.
[92] Y. Koito, H. Imura, M. Mochizuki, Y. Saito, S. Torii, Numerical analysis and experimental verification on thermal fluid phenomena in a vapor chamber, Applied Thermal Engineering, 26 (2006) 1669-1676.
[93] H. Hassan, S. Harmand, 3D transient model of vapour chamber: effect of nanofluids on its performance, Applied Thermal Engineering, (2012).
[94] S.W. Chang, K.F. Chiang, T.H. Lee, Thermal performance of thin loop-type vapor chamber, Experimental Thermal and Fluid Science, 61 (2015) 130-143.

[95] Q. Cai, B.C. Chen, C. Tsai, Design, development and tests of high-performance silicon vapor chamber, Journal of Micromechanics and Microengineering, 22 (2012) 035009.
[96] J.A. Weibel, S.V. Garimella, J.Y. Murthy, D.H. Altman, Design of integrated nanostructured wicks for high-performance vapor chambers, IEEE Transactions on Components Packaging and Manufacturing Technology, 1 (2011) 859-867.
[97] J. Weibel, S. Kim, T. Fisher, S. Garimella, Carbon nanotube coatings for enhanced capillary-fed boiling from porous microstructures, Nanoscale and Microscale Thermophysical Engineering, 16 (2012) 1-17.
[98] A. Melechko, T. McKnight, M. Guillorn, V. Merkulov, B. Ilic, M. Doktycz, D. Lowndes, M. Simpson, Vertically aligned carbon nanofibers as sacrificial templates for nanofluidic structures, Applied Physics Letters, 82 (2003) 976-978.
[99] H.H. Bau, S. Sinha, B. Kim, M. Riegelman, Fabrication of nanofluidic devices and the study of fluid transport through them, in: Optics East, International Society for Optics and Photonics, 2005, pp. 201-213.
[100] B.R. Flachsbart, K. Wong, J.M. Iannacone, E.N. Abante, R.L. Vlach, P.A. Rauchfuss, P.W. Bohn, J.V. Sweedler, M.A. Shannon, Design and fabrication of a multilayered polymer microfluidic chip with nanofluidic interconnects via adhesive contact printing, Lab on a Chip, 6 (2006) 667-674.
[101] A. Han, N.F. de Rooij, U. Staufer, Design and fabrication of nanofluidic devices by surface micromachining, Nanotechnology, 17 (2006) 2498.
[102] G. Peterson, A. Duncan, M. Weichold, Experimental investigation of micro heat pipes fabricated in silicon wafers, Journal of Heat Transfer, 115 (1993) 751-756.
[103] X. Dai, F. Yang, R. Yang, Y.-C. Lee, C. Li, Micromembrane-enhanced capillary evaporation, International Journal of Heat and Mass Transfer, 64 (2013) 1101-1108.
[104] X. Dai, M. Famouri, A.I. Abdulagatov, R. Yang, Y.-C. Lee, S.M. George, C. Li, Capillary evaporation on micromembrane-enhanced microchannel wicks with atomic layer deposited silica, Applied Physics Letters, 103 (2013) 151602.
[105] C. Sobhan, R. Rag, G. Peterson, A review and comparative study of the investigations on micro heat pipes, International Journal of Energy Research, 31 (2007) 664-688.
[106] Y. Wang, G. Peterson, Capillary evaporation in microchanneled polymer films, Journal of Thermophysics and Heat Transfer, 17 (2003) 354-359.
[107] C. Oshman, Q. Li, L.-A. Liew, R. Yang, V.M. Bright, Y. Lee, Flat flexible polymer heat pipes, Journal of Micromechanics and Microengineering, 23 (2013) 015001.
[108] F.E. Bliss, E.G. Clark, B. Stein, Construction and test of a flexible heat pipe, in: Proceedings of ASME Space Systems and Thermal Technologies for the 70's, 1970, pp. 1-7.
[109] R.B. Schweickart, M.M. Buchko, Flexible heat pipes for CCD cooling on the advanced camera for surveys, in: Astronomical Telescopes & Instrumentation, International Society for Optics and Photonics, 1998, pp. 292-300.
[110] D. McDaniels, G.P. Peterson, Investigation of polymer based micro heat pipes for a flexible spacecraft radiator, in: Proc. ASME Int. Mechanical Engineering Congress and Exposition, New York, 2001, pp. 423-433.
[111] C. Oshman, B. Shi, C. Li, R. Yang, Y. Lee, G. Peterson, V.M. Bright, The development of polymer-based flat heat pipes, Journal of Microelectromechanical Systems, 20 (2011) 410-417.
[112] K.-S. Yang, T.-Y. Yang, C.-W. Tu, C.-T. Yeh, M.-T. Lee, A novel flat polymer heat pipe with thermal via for cooling electronic devices, Energy Conversion and Management, 100 (2015) 37-44.
[113] J. Kim, S. You, S.U. Choi, Evaporative spray cooling of plain and microporous coated surfaces, International Journal of Heat and Mass Transfer, 47 (2004) 3307-3315.
[114] K. Paiva, M. Mantelli, Theoretical thermal study of wire-plate mini heat pipes, International Journal of Heat and Mass Transfer, 83 (2015) 146-163.
[115] Y. Wang, Investigation of a novel flat heat pipe, Journal of Heat Transfer, 127 (2005) 165.
[116] J. Ha, G. Peterson, Capillary performance of evaporating flow in micro grooves: an analytical approach for very small tilt angles, Journal of Heat Transfer, 120 (1998) 452-457.
[117] Y.M. Hung, K.-K. Tio, Thermal Analysis of a Water-Filled Micro Heat Pipe With Phase-Change Interfacial Resistance, Journal of Heat Transfer, 134 (2012).
[118] A.K. Mallik, G.P. Peterson, Steady-state investigation of vapor deposited micro heat pipe arrays, Journal of Electronic Packaging, 117 (1994).
[119] K. Knowles, A. Van Helvoort, Anodic bonding, International Materials Reviews, 51 (2006) 273-311.
[120] M. Mihailovic, C. Rops, J. Hao, L. Mele, J. Creemer, P. Sarro, MEMS silicon-based micro-evaporator, Journal of Micromechanics and Microengineering, 21 (2011) 075007.
[121] J. Qu, H.Y. Wu, Silicon-Based Micro Pulsating Heat Pipe for Cooling Electronics, Advanced Materials Research, 403 (2012) 4260-4265.
[122] J. Qu, H. Wu, P. Cheng, Start-up, heat transfer and flow characteristics of silicon-based micro pulsating heat pipes, International Journal of Heat and Mass Transfer, (2012).
[123] A.K. Mallik, G. Peterson, M.H. Weichold, Fabrication of vapor-deposited micro heat pipe arrays as an integral part of semiconductor devices, Journal of Microelectromechanical Systems, 4 (1995) 119-131.
[124] 3M Specialty Fluids, in: http://www.3m.com/market/industrial/fluids/library (ed.), 2006.
[125] C. Sperry, R. Philstrom, P. Claybaker, J. Webster, R. Cree, SS-1 supercomputer cooling system, in: Electronic Components and Technology Conference, 1993, pp. 218-237.

[126] A. Bar-Cohen, M. Arik, M. Ohadi, Direct liquid cooling of high flux micro and nano electronic components, Proceedings of the IEEE, 94 (2006) 1549-1570.
[127] Typical physical properties of common liquids at 293 K, in, http://www.freestudy.co.uk/liquid%20properties.htm.
[128] M. Conde Engineering, in, http://www.mie.uth.gr/ekp_yliko/NH3_H2OProperties_1.pdf, 2004.
[129] J. Qu, H.-Y. Wu, Q. Wang, Experimental Investigation of Silicon-Based Micro-Pulsating Heat Pipe for Cooling Electronics, Nanoscale and Microscale Thermophysical Engineering, 16 (2012) 37-49.
[130] S. Khandekar, N. Dollinger, M. Groll, Understanding operational regimes of closed loop pulsating heat pipes: an experimental study, Applied Thermal Engineering, 23 (2003) 707-719.
[131] P. Charoensawan, S. Khandekar, M. Groll, P. Terdtoon, Closed loop pulsating heat pipes: Part A: parametric experimental investigations, Applied Thermal Engineering, 23 (2003) 2009-2020.
[132] R. Savino, A. Cecere, R. Di Paola, Surface tension-driven flow in wickless heat pipes with self-rewetting fluids, International Journal of Heat and Fluid Flow, 30 (2009) 380-388.
[133] L. Troniewski, R. Ulbrich, Two-phase gas-liquid flow in rectangular channels, Chemical Engineering Science, 39 (1984) 751-765.
[134] J.W. Coleman, S. Garimella, Characterization of two-phase flow patterns in small diameter round and rectangular tubes, International Journal of Heat and Mass Transfer, 42 (1999) 2869-2881.
[135] A. Miner, U. Ghoshal, Cooling of high-power-density microdevices using liquid metal coolants, Applied Physics Letters, 85 (2004) 506-508.
[136] L. Yu, W.Q. Liu, Analysis of the Evaporating Characteristics of the Grooved Micro Heat Pipe with Alkali Metals as Working Fluid, Advanced Materials Research, 516 (2012) 84-87.
[137] S.U. Choi, J. Eastman, Enhancing thermal conductivity of fluids with nanoparticles, in, Argonne National Lab., IL (United States), 1995.
[138] C.T. Nguyen, G. Roy, C. Gauthier, N. Galanis, Heat transfer enhancement using Al2O3–water nanofluid for an electronic liquid cooling system, Applied Thermal Engineering, 27 (2007) 1501-1506.
[139] J. Lee, I. Mudawar, Assessment of the effectiveness of nanofluids for single-phase and two-phase heat transfer in micro-channels, International Journal of Heat and Mass Transfer, 50 (2007) 452-463.
[140] P. Naphon, P. Assadamongkol, T. Borirak, Experimental investigation of titanium nanofluids on the heat pipe thermal efficiency, International Communications in Heat and Mass Transfer, 35 (2008) 1316-1319.
[141] P. Naphon, D. Thongkum, P. Assadamongkol, Heat pipe efficiency enhancement with refrigerant–nanoparticles mixtures, Energy Conversion and Management, 50 (2009) 772-776.
[142] L.G. Asirvatham, R. Nimmagadda, S. Wongwises, Heat transfer performance of screen mesh wick heat pipes using silver–water nanofluid, International Journal of Heat and Mass Transfer, 60 (2013) 201-209.
[143] X.F. Yang, Z.-H. Liu, J. Zhao, Heat transfer performance of a horizontal micro-grooved heat pipe using CuO nanofluid, Journal of Micromechanics and Microengineering, 18 (2008) 035038.
[144] Z.H. Liu, X.F. Yang, G.S. Wang, G.L. Guo, Influence of carbon nanotube suspension on the thermal performance of a miniature thermosyphon, International Journal of Heat and Mass Transfer, 53 (2010) 1914-1920.
[145] Z.H. Liu, L. Lu, Thermal performance of axially microgrooved heat pipe using carbon nanotube suspensions, Journal of Thermophysics and Heat Transfer, 23 (2009) 170-175.
[146] S.H. Noie-Baghban, G. Majideian, Waste heat recovery using heat pipe heat exchanger (HPHE) for surgery rooms in hospitals, Applied Thermal Engineering, 20 (2000) 1271-1282.
[147] A. Faghri, Heat Pipe Science and Technology, Taylor &Francis, US, 1995.
[148] G.P. Peterson, An Introduction to Heat Pipes, in, Canada: John Wiley & Sons, Inc., 1994.
[149] P. Dunn, D.A. Reay, Heat pipes, in, Pergamon Press, Ltd., New York, NY, 1978.
[150] M. Terpstra, J.G. Van Veen, Application of Heat Pipes, Heat Pipe Equipped Heat Exchangers, in: Heat Pipes: Construction and Application, Springer, 1987, pp. 83-363.
[151] R. Revellin, J.R. Thome, A theoretical model for the prediction of the critical heat flux in heated microchannels, International Journal of Heat and Mass Transfer, 51 (2008) 1216-1225.
[152] A. Bergles, S. Kandlikar, On the nature of critical heat flux in microchannels, Journal of Heat Transfer, 127 (2005) 101-107.
[153] L. Bai, G. Lin, H. Zhang, D. Wen, Mathematical modeling of steady-state operation of a loop heat pipe, Applied Thermal Engineering, 29 (2009) 2643-2654.
[154] X. Zhang, X. Zhao, J. Xu, X. Yu, Characterization of a solar photovoltaic/loop-heat-pipe heat pump water heating system, Applied Energy, (2012).
[155] X. Chen, C.K. Wong, C.A. Yuan, G. Zhang, Nanowire-based gas sensors, Sensors and Actuators B, 177 (2012) 178-195.
[156] G.Q. Zhang, A. van Roosmalen, More than Moore: creating high value micro/nanoelectronics systems, Springer, 2009.